Respiratory bioaccessibility and solid phase partitioning of potentially harmful elements in urban environmental matrices

Alexys Giorgia Friol Boim, Carla Patinha, Joanna Wragg, Mark Cave, Luís Reynaldo Ferracciú Alleoni

PII: S0048-9697(20)36320-8

DOI: https://doi.org/10.1016/j.scitotenv.2020.142791

Reference: STOTEN 142791

To appear in: *Science of the Total Environment*

Received date: 6 March 2020

Revised date: 28 September 2020

Accepted date: 29 September 2020

Please cite this article as: A.G.F. Boim, C. Patinha, J. Wragg, et al., Respiratory bioaccessibility and solid phase partitioning of potentially harmful elements in urban environmental matrices, *Science of the Total Environment* (2020), https://doi.org/10.1016/j.scitotenv.2020.142791

Respiratory bioaccessibility and solid phase partitioning of potentially harmful elements in urban environmental matrices

Alexys Giorgia Friol Boim [a, 1, *]

Carla Patinha [b]

Joanna Wragg [c]

Mark Cave [c]

Luís Reynaldo Ferracciú Alleoni [a]

[a] Department of Soil Science, Luiz de Queiroz College of Agriculture (ESALQ), University of São Paulo (USP), 13418-900, Piracicaba, São Paulo, Brazil.

[b] GEOBIOTEC, Geosciences Department, Aveiro University, Campus de Santiago, 3810-193 Aveiro, Portugal.

[c] British Geological Survey, Environmental Science Centre, Nicker Hill, Keyworth, Nottingham NG12 5GG, UK.

* Corresponding author at: Department of Soil Science, University of São Paulo (ESALQ/USP), Av. Pádua Dias, 11, 13418-900, Piracicaba/SP, Brazil. Tel.: +55 19 3417 2155. E-mail address: agfboim@usp.br (A. G. F. Boim).

Abstract

Studies regarding the role of geochemical processes in urban environmental matrices (UEM) and their influence on respiratory bioaccessibility in humans are scarce in humid tropical regions, especially in Brazil. Contaminated UEM are potentially hazardous to humans if particles < 10 µm in diameter are inhaled and reach the tracheobronchial region. In this study, we evaluated samples collected in Brazilian UEMs with a large environmental liability left by former mining industries and in a city with strong industrial expansion. UEM samples were classified into soil, sediment and mine tailings according to the characteristics of the collection sites. The respiratory bioaccessibility of potentially harmful elements (PHE) was evaluated using artificial lysosomal fluid (ALF, pH 4.5), and the BCR-sequential extraction was performed to evaluate how the respiratory bioaccessibility of the PHE was related to the solid phase partitioning. The bioaccessible fraction (BAF) ranged from 54 - 98% for Cd; 21 - 89% for Cu; 46 - 140% for Pb, 35 - 88% for Mn and; 41 - 84% for Zn. The average BAF of the elements decreased in the following order: Soil: Cd> Pb> Mn> Zn> Cu; Tailing: Pb> Cd> Zn> Mn> Cu; and Sediments: Pb> Mn> Cd> Zn> Cu. BCR-fractions were useful to predict the PHE

[1] Current Address: Department of Oceanography and Ecology, Federal University of Espírito Santo, Vitória, Espírito Santo 29075-910, Brazil.

bioaccessibility (R^2 = 0.79 – 0.98), thus suggesting that particle geochemistry and mineralogy can influence PHE behaviour in the pulmonary fluid. Therefore, this approach provides a combination of quantitative and qualitative data, which allows us to carry out a more realistic assessment of the current situation of the potentially contaminated site and possible alternatives for decision making by the stakeholders.

Keywords: Artificial lysosomal fluids; human inhalation exposure; < 10 µm particulate matter; mineralogy; sequential extraction

Funding sources that supported the work

This study was supported by the São Paulo Research Foundation (FAPESP) [grants # 15/19332-9 and # 15/24483-9]; by the Brazilian National Council for Scientific and Technological Development (CNPq) [grant # 404164/2016].

Highlights

- Artificial lysosomal fluid - ALF can estimate the respiratory bioaccessibility of PHE
- The solid phase distribution provided insights into behaviour of PHE in ALF
- The bioaccessibility varied with the geochemical and mineralogical characteristics
- *In vitro* methods should become part of HHRA procedures

Graphical abstract

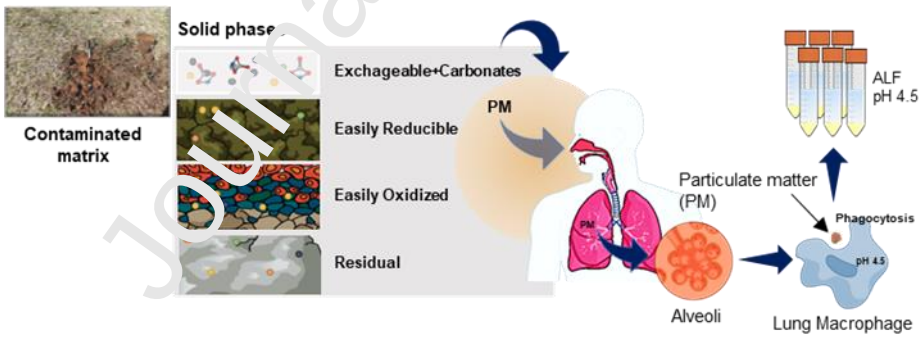

1. Introduction

In the urban environment, potentially harmful elements (PHE) have several sources, such as soils, household dust, vehicular traffic and industrial activity. Urban soils can be a sink of a substantial amount of waste products, including industrial and mining waste and particulate matter emitted by motor vehicles or industrial chimneys whose contaminated particles can be deposited onto the superficial layers of urban soils. Such particulate matter (PM), as fine fraction of soil or dust particles, can subsequently be carried by the wind and reach human respiratory airways.

In the context of human health risk assessment (HHRA), exposure routes are the paths on which contaminants can establish contact with the organism, such as ingestion, dermal contact or absorption and inhalation (USEPA, 1989). Besides, the risk estimate should be determined for each PHE identified at the investigated area, considering the duration of the exposure and the dose-response, that is, the probability that a PHE has to produce adverse effects on the receptors (Jaishankar et al., 2014; Öberg and Bergbäck, 2005).

The risk associated with human exposure to PM can be based on the assumption that inhalation will be the main route reached (Tong et al., 2019; Zhang et al., 2014) either during indoor or outdoor activities. PM is classified into two categories, PM_{10} = aerodynamic diameters <10 µm and $PM_{2.5}$ = aerodynamic diameters < 2.5 µm (USEPA, 2016). According to Kastury et al. (2017), PM10 has a higher risk via inhalation as it can reach the tracheobronchial and alveolar region.

PM_{10} and $PM_{2.5}$ can be suspended in the air for long periods of time, e.g. the PM_{10} can be suspended for a few hours, while $PM_{2.5}$ can remain suspended in the atmosphere for several days to weeks (Leelasakultum and Kim Oanh, 2017) and when inhaled are deposited onto the surfaces of the respiratory system. The inhalation of PM may pose human health in risk by causing various respiratory diseases, such as irritation of the airways, allergic, asthma or others inflammatory reactions and fibrosis (Habybabady et al., 2018; Tong et al., 2019). PM not removed from the body by muco-ciliary clearance, that is, the insoluble particle can be swallowed toward the gastrointestinal tract, may reach the respiratory system becoming susceptible to solubilization by lung fluids (Guney et al., 2016). Thus, PHE exposure risk via inhalation is related not only to the particle size, but also to the type of solid fraction particle that can be easily solubilized in this environment.

The inhaled PM can be transported and trapped in the tracheobronchial system, and PHE bound to the PM can be solubilized by the epithelial lining fluids or extracellular environment. The PHE may be subjected to absorption, and/or diffused within the pulmonary system, even may bind to proteins and some cellular structures reaching the circulatory system (Lehnert, 1990; Oberdörster et al., 2005). When a particle is not solubilized by the epithelial lining fluid, it can be phagocytized by alveolar macrophage (intracellular environment). The presence of enzymes, oxygen radicals, chelating agents and low pH promotes the dissolution of a variety of substances (Kreyling, 1992). In contrast, Galle et al. (1992)demonstrated that the opposite also might occur in the alveolar region, since alveolar macrophages are able to concentrate and precipitate various elements inhaled, preventing the diffusion of toxic substances into the bloodstream.

The respiratory bioavailability of PHE or organic substances has been estimated using *in vivo* tests with animal models, such as rodents (Moreda-Piñeiro et al., 2011), but these models are generally difficult to

reproduce, expensive, time-consuming and have ethical constraints. The *in vitro* methods of respiratory bioaccessibility has been used as a surrogate for *in vitro* tests. The application of lung fluids that simulate the solubilization of the studied material (i.e., PM, dusts) in the respiratory tract and, subsequently, the elemental composition of the leachate were evaluated by Huang et al., 2014; Julien et al., 2011 and Niu et al., 2010.

Respiratory bioavailability is the PHE concentration that crosses the barrier between air and blood reaching the circulatory system, while respiratory bioaccessibility is the PHE concentration solubilized on the lung fluids that lining the respiratory system, but it does not necessarily cross the air-blood barrier, that is, it is considered potentially available to humans (Kastury et al., 2017). Molina et al. (2013) evaluated the bioaccessibility of Zn by simulating synthetic lung fluid, mimicking the phagolysosomal fluid at pH 4.5 (intracellular environment) and the bioavailability assisted by intranasal administration of Zn (from Zn mine waste and minerals) in rodents and observed a positive relationship between the *in vivo* and *in vitro* tests (R^2 = 0.86). However, there is no standardised procedure (Calas et al., 2017; Kastury et al., 2017; Pelfrêne et al., 2017) in which *in vitro* methods can be compared with *in vivo* studies.

These tests have been used to evaluate respiratory bioaccessibility in environmental matrices: Huang et al. (2014), Julien et al. (2011) and Niu et al. (2010) evaluated the respiratory bioaccessibility of PHE from atmospheric particles (i.e. household air-conditioning filter dust, PM2.5, airborne particulate matter). Similarly, Boisa et al. (2014), Drysdale et al. (2012), Guney et al. (2017), Pelfrêne et al. (2017) and Wragg and Klinck (2007) have used these tests to measure the respiratory bioaccessibility of PHE from soil; Colombo et al. (2008) and Witt III et al. (2014) have assessed road dust; oxide nanoparticles have been investigated by Cruz et al. (2015) and Zhong et al. (2017); and pharmaceutical materials have been looked at by Marques et al. (2011) and Tronde (2002).

Simulated lung fluids (SLF), as Gamble's solution, are widely used to simulate the extracellular lung fluids and estimate the concentration of PHE potentially available for absorption via respiratory tract (Drysdale, 2012; Wragg and Klinck, 2007). Another SLF widely used is the artificial lysosomal fluid (ALF), which simulates a more acidic environment (pH value of 4.5, against 7.3 for Gamble solution) and mimics the intracellular conditions in the lungs, i.e., the particle comes into contact with the lung fluids after being phagocytosed by alveolar and interstitial macrophages (Calas et al., 2017; Colombo et al., 2008). The presence of complexing ligands (organic acids) and the low pH in the intracellular environment may release PHE adsorbed to oxides, since the complexation of polyvalent cations with chelating agents (e.g. citrate acid) can increase the mobilisation of PHE in the lung (Calas et al., 2017; Wiseman, 2015).

The SLF may alter the speciation of PHE in the solid fraction of the inhaled matrix. However, the properties of each type of matrix can reflect on the behaviour of a PHE dissolved by the fluid lining in the respiratory system, which led us to hypothesize that the PHE associated with more labile solid phases (soluble and exchangeable) in the soil and those phases associated with Fe oxides or/and organic matter in fine soil particle (< 10 μm) can be released into the pulmonary tract. This highlights the importance of characterizing the mineralogy and the solid phase partitioning of environmental matrices in conjunction with *in vitro* bioaccessibility tests to have a set of quantitative and qualitative data and information to obtain more realistic estimates of risk human health.

Mine tailings, generally, have high concentrations of PHE associated with solid particulate matter (i.e. PM10 or PM2.5) and can be easily carried by winds or water runoff. A large volume of tailing is generated during the ore beneficiation process and, most of the time, they are arranged in places with little or no monitoring plan and inspection. Historical mining disasters in Brazil and worldwide still pose a threat to human and environmental health because of the legacy of associated contaminants. In this study, we collected UEM samples from a Brazilian city with the worst social-environmental disaster associated with mine tailings: the Santo Amaro city, located in the State of Bahia, northeast region of Brazil. In the 1980s, a lead (Pb) smelter operated in the city, producing approximately 900,000 tons of metallic Pb from galena (PbS) concentrate, yielding about 490,000 tonnes of Pb tailings (CETEM, 2012). The tailings material was donated to the locals and to city hall to pave access roads, backyards, streets and public places in the city. The material was also deposited on the soil (open air) and contaminated groundwater and the Subaé River (de Andrade Lima and Bernardez, 2011; de Andrade and Moraes, 2013). The magnitude of the result in complex effects on the environment, and the society often does not have adequate answers about how much and how long they directly affect the health of the exposed population. Therefore, studies of urban soils in areas that were previously associated to some industrial activity are necessary. Principally, for those sites that have been abandoned (commonly called, *brownfields*), and are contaminated or with suspected of contamination, because humans can be exposed directly to the soil surface and windblown materials or dust.

In vitro bioaccessibility methods give an estimate of hazard exposure and provide a line of evidence for HHRA. Such information can inform adequate management of contaminated land relative to the risk of population exposure to health hazards (Cave, 2012). This study presents the results of *in vitro* respiratory bioaccessibility testing of PHE (Cd, Cu, Pb, Mn and Zn) from a set of soil, tailings and sediment samples collected in three Brazilian cities. These samples had contrasting chemical, physical and mineralogical attributes

and a wide range of total PHE concentrations. The influence of solid-phase partitioning on the PHE bioaccessibility was investigated by coupling *in vitro* and sequential extraction methods. This is the first study involving respiratory bioaccessibility carried out on particulates from the Brazilian urban environment. Thus, it is expected to serve as a reference or recommendation for the use of *in vitro* methods as part of HHRA procedures and could help in the development of public policies by environmental agencies and other stakeholders to evaluate potentially contaminated areas.

2. Material and Methods

2.1 Collection and sampling areas

To understand the inhalation bioaccessibility and solid phase partitioning of bioaccessible PHE within environmental matrices (soils, sediments and mining tailings) samples of urban environmental matrices were collected in three Brazilian cities. The selection of samples was taken at random to obtain a set of heterogeneous samples with contrasting physical, chemical and mineralogical characteristics.

The samples were collected from the cities of Piracicaba (n = 3), the eastern region of the state of São Paulo (SP), Brazil; Apiaí (n = 5), Upper Ribeira Valley (SP); and Santo Amaro (n = 9), in the concave region (Recôncavo Baiano), state of Bahia (BA), Brazil (Table 1 and Figures S1, S2 and S3 (Supplementary Material)). In Piracicaba, soil samples were collected from Mario Telles Square, José Bonifácio Square and at the athletics track of the Luiz de Queiroz College of Agriculture, University of São Paulo, near Independência Avenue, one of the busiest roads in the city (Table 1, Fig. S1). All are recreational sites in residential areas frequented by children but are also characterized by high traffic density.

The samples from Apiaí were collected from the Centre for Integrated and Multidisciplinary Studies of Apiaí (CIEM), a unit of the Mineral Resources Research Company (CPRM) of Geological Survey of Brazil, located in the Upper Ribeira Valley Region (Table 1, Fig. S2). A Pb and silver (Ag) foundry and an old slag deposit operated in this area (Calabouço Mill) from 1940 to 1956. The main environmental issues in this area are mineral dust, metallic waste and Pb slag deposits (Martins and Figueiredo, 2014). The samples were collected from five sites: four in the CIEM area containing soil associated with Pb tailings (Fig. S2) and were classified as mining tailing contaminated; other one was collected in the native forest near the unit and was classified as soil. The sampling locations were selected based on a metal distribution map from a study carried out by Martins and Figueiredo (2014).

In Santo Amaro, the identification of suitable sample collection sites was based on the "Map of soil

contamination by chemical elements in Santo Amaro da Purificação" (Carvalho et al., 2010). Samples were collected from within the city perimeter, including the former lead smelter, which ceased activity in 1993 (CETEM, 2012). People who worked or lived in Santo Amaro during the operational period of the company indicated where the slag was deposited. A total of nine samples were collected: one tailing (collected in the deactivated plant area), four soils (samples collected in residential areas, mainly frequented by children) and four sediments (two samples collected on the banks of the Subaé river and the other two samples collected into a street gutter and in an unpaved road close to the plant area) (Table 1, Fig. S3). Samples classified as sediments commonly had high sand contents (2SA and 3SA) and contained some materials possibly derived from the old Pb metallurgical (7SA and 8SA) operations.

Each sample was composed of five subsamples collected from the 0-5 cm layer (across an area of approximately 4 m²) using a stainless-steel shovel and thoroughly mixed to obtain approximately 5 kg of soil. The samples were then placed in plastic bags and transported to the laboratory. The depth of 0-5 cm was chosen because it is assumed that this is the soil layer that can be carried by the wind and thus can cause risk to human through inhalation/ingestion pathways (Drysdale et al., 2012). The samples were air dried, sieved to < 2 mm, coned and quartered to provide a representative sample for further chemical, physical and mineralogical analyses. Each sample was stored in plastic pots and classified according to the type of matrices: soil, sediment and tailings. This classification was necessary to allow the evaluation of the effect of ALF solution on different matrices.

Table 1. Identification of urban environmental matrices, coordinates and sites characteristics of the local collection of soil, sediments and tailing matrices

#ID	Classification	City	Coordinate		Site
35PC	Soil	Piracicaba	22°42.054'S	47°40.072'W	Mario Telles Square and Playground
47PC	Soil	Piracicaba	22°43'27"S	47°38'52.94"W	José Bonifácio Downtown Square
58PC	Soil	Piracicaba	22°42.850'S	47°37.975'W	Athletics track of the Luiz de Queiroz College of Agriculture campus
3SA	Soil	Santo Amaro	12°33.111'S	38°42.514'W	Saudade Cemetery Garden
5SA	Soil	Santo Amaro	12°33.287'S	38°41.675'W	Neighbourhood Derba, residential area

6SA	Soil	Santo Amaro	12°32.406'S	38°43.637'W	Soccer field for children near the old company facilities
9SA	Soil	Santo Amaro	12°33.651'S	38°42.073'W	Garden of Municipal School Maria dos Anjos Salles Brasil
5AP	Soil	Apiaí	24°32.443'S	48°49.851'W	Native forest, next to the old company facilities
2SA	Sediment	Santo Amaro	12°32.804'S	38°42.491'W	Subaé riverbank, next to Pedro Lago School
4SA	Sediment	Santo Amaro	12°33.019'S	38°42.385'W	Subaé riverbank, near the Forum
7SA	Sediment	Santo Amaro	12°32.427'S	38°43.622'W	Unpaved road connecting Rui Barbosa Avenue and the old facilities
8SA	Sediment	Santo Amaro	12°32.415'S	38°43.602'W	Street gutter of Rui Barbosa Avenue
1AP	Tailing	Apiaí	24°32.315'S	48°49.991'W	Soil with slag from the landfill at old company facilities
2AP	Tailing	Apiaí	24°32.323'S	48°49.909'W	Soil with slag from the landfill at old company facilities
3AP	Tailing	Apiaí	24°32.356'S	48°49.955'W	Soil with slag from the landfill at old company facilities
4AP	Tailing	Apiaí	24°32.349'S	48°49.899'W	Soil with slag from the landfill at old company facilities
1SA	Tailing	Santo Amaro	12°32.371'S	38°43.855'W	Soil with slag from the landfill at old company facilities

2.2 Preparation of the samples for the *in vitro* test

The main interest was focused on particles with aerodynamic diameter of < 10 µm because these particles affect the tracheobronchial system and can reach the alveolar region (Boisa et al., 2014; Guney et al., 2017). Samples for respiratory bioaccessibility testing were prepared by mechanically shaking the 2 mm size fraction through a series of 1 mm, 500 µm, 250 µm, 125 µm and 63 µm (18, 35, 60, 120 and 230 Mesh) sieves for 30 min. The resulting material was retained in a collector and stored in plastic pots prior to further separation

to obtain the 10 µm fraction. All materials used were plastic, except for sieves, which were made of stainless steel, to avoid contamination.

The separation method was adapted from Lijung et al. (2011, 2008). Approximately 40 g of the < 63 µm sub-sample was transferred to a 600 mL beaker containing 500 mL of ultrapure water (18 ΩM cm^{-1}). The suspension was shaken by hand, followed by ultrasonic dispersion for 5 min (three times), allowed to stand for 10 min and filtered using a 10 µm aperture nylon filter with the aid of a vacuum pump. The supernatant was transferred to a beaker and dried at 60 °C for three days. After drying, samples were gently disaggregated using an agate pestle and mortar, stored in plastic pots previously washed with 10% HCl and rinsed with ultrapure water.

The amount of material filtered at 10 µm varied between the samples ranged from 1 to 12 g (data not shown). This fraction was nominated as "fine fraction" or "FF" (diameter < 10 µm) to differentiate it from bulk sample (BS), that is, the sample as a whole (< 2 mm).

2.3 Chemical and physical characterization of bulk samples (BS)

The samples were characterized as follows: pH in water (1:2.5, m/v), granulometric fractions by densimeter, both methods described by Donagema et al. (2011); Total carbon (TC) concentration was determined by catalytic combustion oxidation at 900ºC and measured by a non-dispersive infrared sensor (NDIR) in a Total Organic Carbon Analyzer, model TOC-L (Shimadzu), coupled in a sampler for solid samples SSM 5000A, Shimadzu. The determination of pseudo-total concentration of PHE was carried out in triplicate after acid extraction assisted by a microwave according to method USEPA 3051A (1:3 HCl: HNO_3, v/v) (USEPA, 2007), in both fractions, BS (determined by optical emission spectroscopy with inductively coupled plasma (ICP-OES)) and FF (determined by inductively coupled plasma mass spectrometry (ICP-MS)).

2.4 Determination of respiratory bioaccessibility of PHE in the soil, sediment and tailings matrices

To simulate the intracellular conditions in lung fluids, an ALF solution was prepared as described in Pelfrêne et al. (2017). For this purpose, 0.05g (± 0.0001) of the FF was weighed in 85 mL polycarbonate centrifuge tubes, and 50 mL of the simulated fluid (ratio - 1:1000) were added. This ratio was one of those studied by Pelfrêne et al. (2017), who observed that bioaccessibility does not depend on the soil: solution ratio from 1:1000 to 1:10000.

Samples were shaken at 37 ºC on an end-over-end shaker for 24 h and centrifuged at 4500 × *g* for 15

min. This extraction time was chosen because Cruz et al. (2015), Pelfrêne et al. (2017) and Guney et al. (2017) have shown that it is enough for maximum dissolution of the soil PHE. The extracts were diluted 1:10 with 2% HNO_3 and transferred to polypropylene tubes and kept under refrigeration until determination in ICP MS. For each element, the bioaccessible fraction (BAF%) for the lung compartment was calculated according to the following equation:

$$BAF\ (\%) = \frac{ALF_{conc}}{FF_{pseudototal}} \times 100$$

where: ALF_{conc} = respiratory bioaccessible PHE concentration extracted by ALF (mg kg^{-1}) and $FF_{pseudototal}$ = PHE pseudo-total concentration of the fraction of < 10µm (FF) (mg kg^{-1})

2.5 Sequential Extraction

The BCR-modified method (Rauret et al., 1999) has been successfully applied in studies with several environmental matrices such as soils, sediments and dust (Kasemodel et al., 2019; Lu and Kang, 2018; Unda-Calvo et al., 2017; Zhao et al., 2018). The sequential extraction was performed according to Rauret et al. (1999) in three steps. For this, 0.5 g of FF sample was weighed, instead of 1 g as described by Rauret et al. (1999), and the solid:volume ratio maintained. This was done because of limitations in the amount of FF samples obtained (Section 2.2). To perform sequential extraction, steps were carried out as follows:

(i) F1: the soluble, exchangeable phase (non-specifically adsorbed species) and carbonate-bounded fraction, extracted with 20 mL of 0.11 mol L^{-1} CH_3COOH and shaken for 16h on an end-over-end shaker at room temperature;

(ii) F2: reducible phase, i.e., bound to the Fe and Mn oxides and oxyhydroxides, extracted with 20 mL of 0.5 mol L^{-1} $NH_2OH.HCl$ and shaken for 16h at room temperature; and

(iii) F3: oxidizable fraction, i.e., bound to organic matter and sulphides, extracted with 5 mL of hydrogen peroxide (300 mg g^{-1}, 8.8 mol L^{-1}) with occasional manual shaking during 1h. The digestion was continued for 1 h at 85 ± 2 ° C in a water bath to allow the sample volume to reduce to <3 ml. This step was repeated twice. Then, 25 mL of 1 mol L^{-1} ammonium acetate (pH 2 adjusted with concentrated HNO_3) was added to the residual material and stirred for 16h at room temperature.

All the supernatants were separated from solid sample by centrifugation for 20 min at 3000 x *g and* preserved under refrigeration at 4ºC prior to analysis. The residual solids were then washed with 10 ml of ultrapure water (18 ΩM cm^{-1}), shaken for 15 min and centrifuged for 20 min at 3000 x *g*. The "washing" supernatants were discarded, taking care not to discard the solid residue.

The residual fraction was calculated according to equation: F4 = $FF_{pseudototal}$ (mg kg^{-1}) - Σ[F1, F2, F3 (mg kg^{-1})] (Abdu et al., 2012; Puga et al., 2016). The residual fraction is associated with the elements strongly adsorbed to the crystalline matrix, mainly by specific adsorption, suggesting predominantly a geogenic origin (Patinha et al., 2015).

2.6 Quality assurance and control

The determination of the PHE concentration was performed by Inductively Coupled Plasma Atomic Emission Spectroscopy (Thermo Scientific iCAP 6300 Duo, ICP OES) for the determination of the pseudo-total concentrations of the PHE of the BS and the PHE concentrations of the fractions of the sequential extraction. Inductively Coupled Plasma Mass Spectrometry (Agilent 7700x, ICP-MS) was used to determine the pseudo-total and bioaccessible PHE concentrations, both from the FF samples.

For quality assurance and control, samples of standard reference material (SRM) NIST 2711a (NIST, 2009) were included in the pseudo-total (BS samples) digestion (n = 2) and a SRM BCR 723 (Road Dust) sample was used in the pseudo-total extraction (FF samples) and bioaccessibility procedures (n = 2) (Table S1). Mean recoveries for the selected elements in all SRMs varied from 70 - 126%, and relative standard deviations (RSDs) for all replicates were < 10%. The analytical blanks contained PHE concentrations below the limit of quantification (LQ): 0.005 (Cd, Cu and Mn), 0.01 (Pb), 0.05 (Zn) mg L^{-1} (ICP OES) and 0.003 (Cd and Cu), 0.03 (Pb), 0.1 (Mn), 0.004 (Zn) mg L^{-1} (ICP-MS).

All tests were performed with ultrapure water (18.2 MΩ). All plastic and glassware used was washed with Extran® detergent (3 %) and rinsed with deionized water followed by soaking in 10% HCl for 24h. Finally, all equipment was rinsed with deionized water followed by ultrapure water and placed in an oven to dry at 45 °C.

2.7 X-ray diffraction

All BS (bulk samples (< 2 mm)) were ground in a tungsten mill and sieved to < 100 µm for the identification of the crystalline materials in the urban matrices.

The clay fraction was analysed after treatment with sodium dithionite-citrate-bicarbonate solution (DCB) to eliminate the crystalline Fe oxides and consequently concentrated the silicates in the sample soils. The clay samples were then treated as follows: (i) magnesium (Mg) saturation and air drying to distinguish between the expansive and non-expansive 2:1 minerals; (ii) Mg saturation and glycerol solvation to differentiate

vermiculites from smectites (2:1 minerals); (iii) saturation with potassium (K),air drying and heating to 110, 350 and 550 °C in a muffle to differentiate chlorite from interstratified minerals, 2:1 and 2:2 minerals and for the destruction of 1:1 minerals, such as Kaolinite (Dixon and Weed, 1989).

The mineralogical identification was performed by X-ray diffraction (XRD) using a Philips PW 1877 diffractometer operated at a potential of 40 kV, 40 mA currents, CuKα (k = 1.54186 Å), with a monochromator for the elimination of Kβ radiation, and step increment of one second for each 0.02º (2θ). The samples were deposited on glass slides or a sampler holder and analysed in a scanning range of 3º to 65º (2θ).

2.8 Statistical Analyses

The SPSS Statistics 20 (SPSS Inc.) software was used for descriptive statistics and for parametric and non-parametric tests. The non-parametric tests Kruskal-Wallis and Wilcoxon-Mann-Whitney were chosen rather than ANOVA, because of their better applicability for small samples size ($n < 30$) with groups of different sizes (Marôco, 2011). As the sample size was < 50 the Spearman correlation was used to evaluate the degree of correlation between the variables. Simple (SLR) and multivariate (MLR) linear regression were used to evaluate the relative impact of PHE pseudo-total concentrations and sequential extraction fractions as predictors of PHE bioaccessibility.

The significance of the regression parameters was verified by the F-test ($p < 0.05$). The assumptions of linear regression were verified by the tests of multicollinearity, homoscedasticity, normality and independent errors (Durbin-Watson test). The MLR model was developed by the *stepwise* selection method. The data were log-transformed to normalize their distribution. The logarithmic data were again submitted to the analysis of compliance with the assumptions of the MLR to verify whether the transformation was efficient in adapting the variable to the violated assumption.

3. Results and discussion

3.1 Sample characterization

The chemical and physical characteristics determined in the BS (2mm) are summarized in Table 2 and in the whole dataset in the Supplementary Material (Table S2). The pH varied from 4.2 to 7.1, wherein, soils pH had greater variation (4.2 to 7.1) as compared to sediment (6.6 to 7.1) and tailing (5.2 to 6.6) sets. The total carbon (TC) variation was smaller in the sediments (0.5 to 1.3%) compared to the soils (0.8 to 6.3%) and tailings (0.6 to 3.4%). The median content of clay, silt and sand were similar between the three sample types. According

to FAO (2014) textural classification the samples were classified as sand, loamy sand, sandy loam, sandy clay loam, clay loam, sandy clay and clay.

The samples showed diverse characteristics as expected, even those samples collected from the same city. Random sites were chosen for sampling, and the collection was carried out in the most superficial soil layer (5 cm), that is usually disturbed by anthropogenic activities. Soils from urban areas may have received various inputs from unknown sources over the years, which may be accumulated in the first centimetres, except for the samples classified as tailings, in which all samples were collected from old landfills slag of the galena beneficiation.

Pseudo-total concentration of PHEs in the BS and FF samples varied greatly (Fig. 1 and Table 2), with the highest concentrations found in the samples collected in the mine tailings areas in the city of Apiaí, with concentrations > 1% for some elements, particularly Pb 8% (BS) and 6% (FF) in sample 1AP (Table S2). The Wilcoxon test showed that the concentrations in BS and FF differed for Cu ($Z = -2.58$; $p = 0.01$) and Cd ($Z = -2.63$ $p = 0.009$), where Cu had a higher median in FF (52.2 mg kg^{-1}) than in BS (69.7 mg kg^{-1}), while Cd had a higher median in BS (14.1 mg kg^{-1}) than in FF (4.6 mg kg^{-1}, Fig. 1, Table 2). Commonly, PHE tend to accumulated in fine fraction probably due to the greater specific surface area that provides higher cation adsorption (Luo et al., 2011), but the opposite was observed for Cd, mainly in the tailing samples (Table S2) in which the concentration and distribution of PHE were not only related to tailings particle size fraction, but probably related to the mineralogical composition as well, as phyllosilicates and Fe oxy-hydroxides (Wei et al., 2015).

Cd had the highest pseudo-total concentrations in the BS in most of samples (Tables 2 and S2). A positive correlation was found between Cd and silt (($r = 0.671$, $p < 0.001$) and between Cd and organic carbon (C-org) ($r = 0.486$, $p < 0.05$) and a negative correlation between Cd and sand ($r = -0.547$, $p < 0.05$) in the BS samples (data not shown). This infers that the Cd concentrations could be directly related to silt size (63 to 2 µm). The occurrence of components from organic matter could serve as silt particle coating and generate Cd adsorption sites.

Table 2 Chemical and physical characterization, pseudo-total and bioaccessible concentrations of potentially harmful elements (PHE) of samples collected in urban regions in Brazil.

Parameters	Particle size	Minimum	Maximum	Percentiles		
				25th	50th (Median)	75th

Chemical and Physical characterization						
pH	2 mm	4	7	6	7	7
C-total (%)	2 mm	1	6	1	2	3
Sand (%)	2 mm	18	90	33	56	69
Silt (%)	2 mm	4	29	11	18	27
Clay (%)	2 mm	6	55	16	25	40
Pseudo-total concentration						
Cd (mg kg^{-1})	2 mm	<0.1	134.0	3.5	14.1	21.8
Cu (g kg^{-1})	2 mm	<0.1	21.1	<0.1	0.1	0.3
Mn (g kg^{-1})	2 mm	0.1	1.9	0.2	0.4	0.9
Pb (g kg^{-1})	2 mm	<0.1	82.5	0.1	0.7	7.0
Zn (g kg^{-1})	2 mm	<0.1	11.6	0.1	0.5	3.5
Cd (mg kg^{-1})	10 µm	0.2	122.0	0.6	4.6	12.5
Cu (g kg^{-1})	10 µm	0.1	22.5	0.1	0.1	0.4
Mn (g kg^{-1})	10 µm	0.3	1.2	0.5	0.6	0.8
Pb (g kg^{-1})	10 µm	0.1	67.7	0.2	0.4	6.0
Zn (g kg^{-1})	10 µm	0.1	15.7	0.4	0.6	3.5
Bioaccessible concentration						
Cd (mg kg^{-1})	10 µm	0.2	98.5	0.5	4.2	10.7
Cu (g kg^{-1})	10 µm	<0.1	20.0	<0.1	0.1	0.3
Mn (g kg^{-1})	10 µm	0.2	0.9	0.3	0.4	0.6
Pb (g kg^{-1})	10 µm	<0.1	60.7	0.2	0.4	5.4
Zn (g kg^{-1})	10 µm	<0.1	9.9	0.2	0.5	2.7

For the other elements (Pb, Mn, and Zn) there was no difference ($p > 0.05$), shown by the Wilcoxon test between BS and FF. PHE can be associated with either Fe and Mn oxides or aluminosilicate minerals and incorporated into the structure of minerals present in coarser soil fractions (Batista et al., 2018). Batista et al. (2018) found Pb associated with Fe and Mn, such as plumboferrite [$Pb_2Mn^{2+}_{0.2}Mg_{0.1}Fe^{3+}_{10.6}O_{18.4}$], and primary minerals, such as trioctahedral mica. These authors also found Pb minerals, cerussite ($PbCO_3$), magnetoplumbite [$Pb_{1.1}Fe^{3+}_{7.7}Mn^{3+}_{2.6}Mn^{2+}_{0.6}Ti_{0.6}Al_{0.4}Ca_{0.1}O_{19}$], humboldtine [$Fe^{2+}(C_2O_4)\cdot 2(H_2O]$) and plumbogummite

$[PbAl_3(PO_4)_2(OH)_5 \cdot H_2O]$ in sand and silt fractions, particle size > 2 µm.

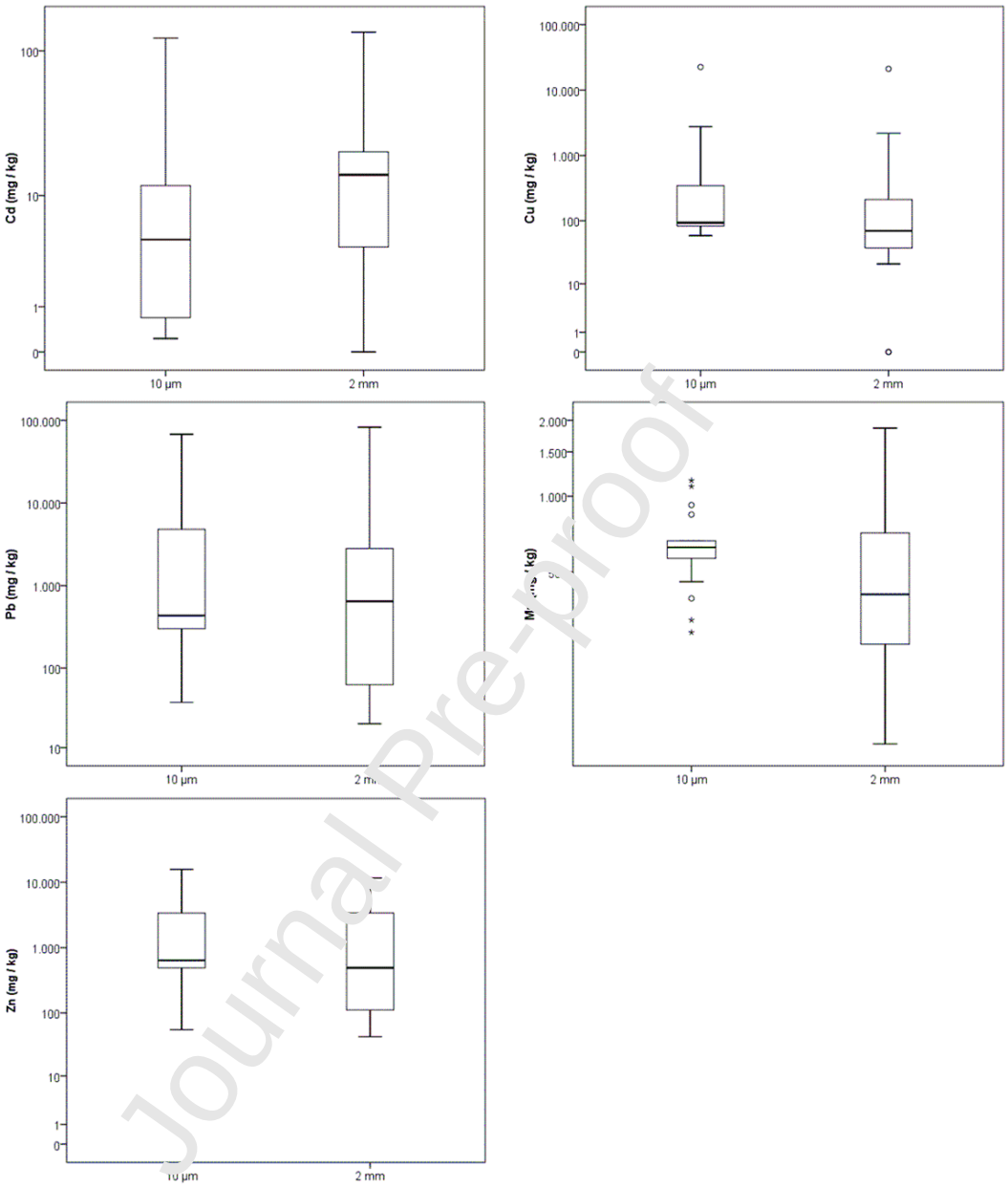

Figure 1 Distribution of potentially harmful elements in the bulk sample (2mm) and fine fraction (10µm) of the urban environmental matrices. Data has been log-transformed for better visualization.

The main minerals identified by XRD in all clay fractions from BS were kaolinite, with illite-montmorillonite, gibbsite and calcite found in smaller amounts (Figure 2). In sample 1AP (tailing), peaks (0.315 and 0.307 nm) corresponding to lead oxide (PbO) were observed. XRD analyses were not performed on the FF samples due to small amount of material available. The concentrations of Cu and Zn are relatively high in tailing samples (Table S2); however no crystalline phases associated with these elements were found, but it can be inferred that these elements are in the form of amorphous oxides or insoluble precipitates, probably due to

sample pH (5.2 to 6.6). Peaks of kaolinite and small amounts of minerals 2:1 and gibbsite were observed in the soil and sediment samples (Figure 2).

Although the PHE concentrations in BS and FF were not different ($p > 0.05$) for most elements, the bioaccessibility and fractionation analyses were performed on FF, since this fraction has a greater potential risk to humans, mainly when inhaled (Witt et al., 2014).

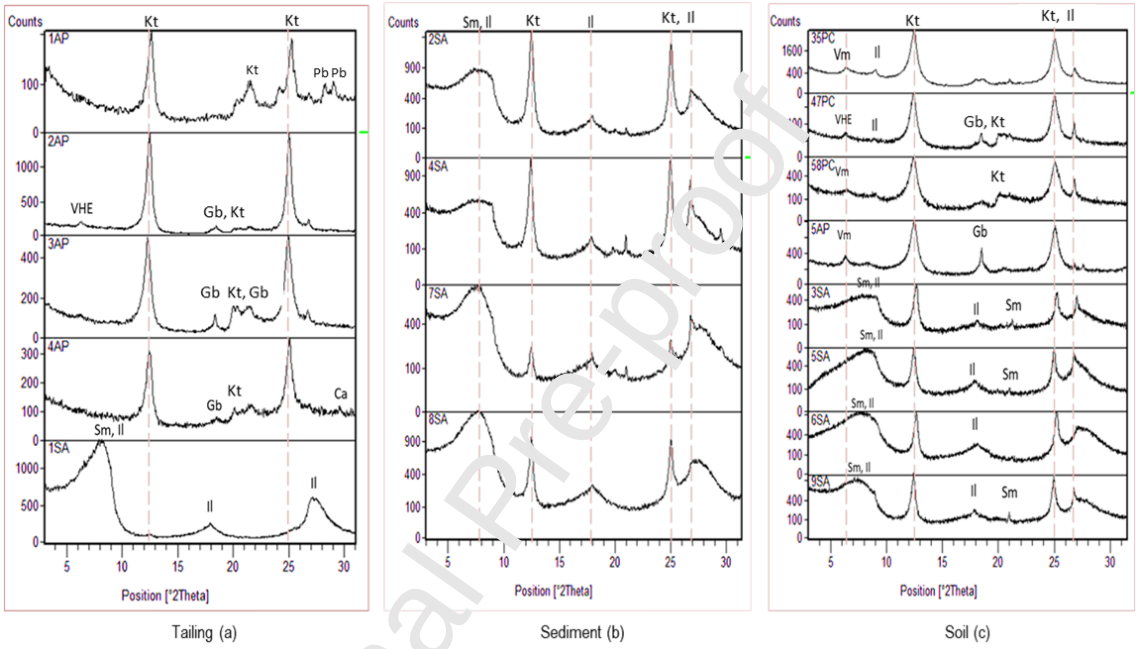

Figure 2 X-ray diffraction of urban environmental matrices - Kaolinite (Kt), Gibbsite (Gb), Smectite mineral group (Sm), Illite (Il), Calcite (Ca), Vermiculite (Vm), Hydroxy-interlayered Vermiculite (VHE), Lead oxide (Pb)

3.2 Respiratory bioaccessibility of PHE in different environmental matrices

The bioaccessible PHE concentration varied widely among matrices, indicating that they were influenced by the chemistry, physical and mineralogical characteristics, as well as the land uses of the sample matrix (Table 1 and S2). The median bioaccessible concentration were 0.5 (Cd); 31 (Cu); 193 (Pb); 325 (Mn) and 239 (Zn) mg kg^{-1} for the soil matrix; 5 (Cd); 49 (Cu); 648 (Pb); 512 (Mn); and 482 (Zn) mg kg^{-1} for the sediment matrix, and 11 (Cd); 950 (Cu); 416 (Mn) mg kg^{-1}; and 3 (Zn) and 10 (Pb) g kg^{-1} for the tailing matrix (data not shown).

The tailing matrix, as expected, had the highest bioaccessible concentrations of PHE, but some soil (6SA) and sediment (8SA) samples collected in Santo Amaro also had high levels of bioaccessible Cd (20 and

12 mg kg^{-1}), Pb (4,812.1 and 2,014.7 mg kg^{-1}) and Zn (2,516.9 and 1,849.0 mg kg^{-1}) compared to the housing investigation value (IV-H) of regulatory guidance from Brazilian National Environment Council (CONAMA) (Resolution # 420, 28/12/2009,(CONAMA, 2012)) established for soils in residential areas (8, 300 and 1000 mg kg^{-1}, respectively). The Brazilian intervention values were derived based on generic scenarios (agricultural, housing and industrial) considering characteristics of the physical environment, human behaviour and length of stay in the site. In addition, the methodology includes exposure pathways for each substance present in the soil, such as ingestion and inhalation of soil particles (Dias et al., 2006).

According to CONAMA #420/2009, concentrations of PHE in soils above the IV-H may present direct or indirect risks to human health and that the fulfilment of requirements for the contamination control should be made for hazard elimination or reduction. Even though the bioaccessible respiratory concentration was determined in the FF samples, we compared the results with the IV-H established by CONAMA, as there is no protocol in the country that adopts *in vitro* bioaccessibility methods as a requirement for an HHRA.

Samples 6SA and 8SA were collected from a soccer field and the sidewalk located on an avenue near an old of Pb metallurgical facility. The presence of these elements at these sites is probably associated with a flood that occurred in 2015, prior to soil collection, when several particulates and coarse materials, derived from the plant, were transported to the sites. The sample sites are less than 1 km from the old company and these results might indicate serious contamination due to the particulate material in this region. These data suggest a potential concern in the area, and more detailed assessments of risks to human health are needed.

Median bioaccessible fractions (BAF) in the tailing samples were Pb (90%) > Cd (87%) > Zn (78%) > Mn (63%) > Cu (61%), in soils: Cd (77%) > Pb (73%) > Mn (69%) > Zn (55%) > Cu (47%) and in sediments: Pb (86%) > Mn (84%) > Cd (79%) > Zn (71%) > Cu (56%) (Figure 3). As for Pelfrêne et al (2017), respiratory bioaccessibility was influenced by the composition of the matrices, such as oxides, carbonates, aluminate, phosphate and silicate, as well as the chemical behaviour of each element and its ability to form soluble complexes with ALF components. The high % bioaccessibility (> 50%) was observed for all elements in the most of samples (Figure 3). This was expected, since the ALF is an aggressive solution because of its low pH (4,5) and the presence of chelating agent able to dissolve some PHE components.). Pelfrêne et al. (2017) observed that the bioaccessibility of the elements was higher using the ALF compared to the other simulated fluids and concluded that ALF solution could be used to assess the lung bioaccessibility of PHE because it provides a more conservative estimation of the bioaccessible PHE.

The Kruskal-Wallis non-parametric test ($p > 0.05$) was conducted to evaluate the differences in PHE

respiratory bioaccessibility according to the matrices. The BAF medians did not differ between all three matrices, except for Mn, (H (2) = 7.482, p = 0.024), in which the sediment group differed from the soil and tailings matrices. This is likely to be related to mineralogy of sediment samples, where there is predominance of 2:1 mineral (Figure 2). These samples had similar mineralogical composition in the clay fraction (Figure 2b). XRD analysis identified the phyllosilicates minerals in the four samples, with Mica group minerals (ex., Illite (Il)), Smectites group minerals (Sm), both are 2:1 mineral, and Kaolinite (Kt), which is 1:1 mineral.

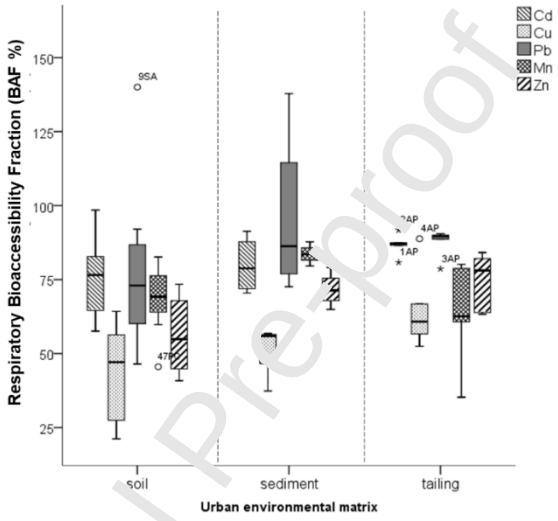

Figure 3. Box and whisker plot of the respiratory bioaccessible fraction (BAF %) of Cd, Cu, Mn, Pb and Zn separated by type of matrix (Sediments (n = 4). Soil (n = 8) and Tailings (n = 5)). Asterisks are mean extremes, and degree signs are outliers.

These results might imply that mineral phase controls the Mn bioaccessibility because the 2:1 clay minerals have a large surface area and high cation exchange capacity, thus allowing high PHE sorption (Lamb et al., 2009). Besides that, Mn is present in soils and sediments mainly in the form of oxides and hydroxides and can be easily solubilized and incorporated into weathering products from soils (Gilkes and McKenzie, 1988). Other factors may affect the dynamic of Mn on ALF fluids, such as pH and redox reaction that occurs in the matrix (Hedberg et al., 2011). Similar Mn bioaccessibility (89%) was found by Hernández-Pellón et al. (2018) in PM_{10} from a urban-industrial site in the north of Spain using ALF fluid. One of the ALF components is the citric acid (20.8 g L^{-1}) which is able to reduce Mn (IV) to Mn (II) and make it soluble. The citric acid is a tricarboxylic organic acid that promotes the dissolution of Mn oxides, mainly amorphous oxides (Hedberg and Odnevall Wallinder, 2016) and is able to dissolve secondary minerals, such as kaolinite and 2:1 minerals (Ramos et al.,

2011), because of the high metal complexation capacity of the carboxyl group.

Mn is one of the elements not included in the table of background guideline values for Brazilian soils (CONAMA, 2012), although it is essential for humans for the synthesis and metabolism of neurotransmitters (Dieter et al., 2005). Prolonged exposure to fumes and dust containing high concentrations of Mn represents a risk factor for diseases such as Parkinson's (Kwakye et al., 2015) or Alzheimer's (Tong et al., 2014), as well as diseases associated with pulmonary inflammation (Santamaria and Sulsky, 2010). Studies on the contamination of soils or dust by Mn and its effects on human health have not been considered so far in Brazil. According to the USEPA (USEPA, 1995), the reference dose for Mn is 10 mg day^{-1} (or 0.14 mg kg^{-1} day^{-1} for 70 kg adults) for chronic ingestion and the inhalation lowest-observed-adverse-effect level (LOAEL) is 0.793 mg m^{-3}. Neurotoxicity has been reported in environments where there is chronic exposure containing > 1 mg m^{-3} of Mn (Santamaria and Sulsky, 2010). As such, further studies focussed on Mn exposure are required, especially on the dose-effect relationship (Santamaria and Sulsky, 2010).

Extraction with ALF fluid resulted in PHE proportions (BAF) equal to or greater than 100% in some samples (Figure 3). This was probably because the ALF solution is a complex medium with a high concentration of organic complexes, low pH (4.5) and is able to solubilize high concentrations of these elements (Pelfrêne et al., 2017). Moreover, the high solid: solution ratio (1:1000) used in the procedure, unlike the solid: solution ratio in the 3051A method (1:24), can contribute to a greater dissolution of the < 10 µm material (Guney et al., 2017). Therefore, it is suggested that the pseudo-total concentration in these cases should be interpreted with caution for risk assessment. The high release of bioaccessible PHE in the different matrices is due to the high complex forming capacity of the solution that contains six types of organic chemical substances (0.077 g L^{-1} trisodium citrate dihydrate, 0.059 g L^{-1} Glycine, 20.8 g L^{-1} Citric acid, 0.090 g L^{-1} disodium tartrate, 0.085 g L^{-1} sodium lactate and 0.172 g L^{-1} sodium pyruvate).

The release of PHE may increase with an increase in the capacity to form stable complexes and the concentration of ligands in the solution (Hedberg et al., 2011). The effect of pH alone is not as significant as the action of organic complexing agents and the number of available functional groups (Hedberg et al., 2011). The presence of citric acid and other organic substances in the ALF fluid promotes the formation of complexes with the metals, resulting in increased solubility, thus replacing the adsorbed metals on the surface of the particulate matter and forming organometallic complexes in the ALF solution (Henderson et al., 2014; Kim et al., 2013).

3.3 Influence of solid phase matrices in the respiratory bioaccessibility of potentially harmful elements

3.3.1 Sequential extraction

A high variability of the geochemical phases in the soil, sediment and tailing matrices was observed in the sequential extraction (BCR) results for all elements studied (Fig. 4 and S4). In the tailing samples, the PHE most associated with the F1, that is the mobile phase and bound to carbonates of the environmental matrices, were Mn, Cd and Zn (median 30, 44 and 51%, respectively) compared to the other elements studied (Figure 4). High concentrations of carbonates are generally found in environmental matrices with pH > 6 (Hooda, 2010). In this case, the PHE would be associated or precipitated with carbonated minerals that may be dissolved by 0.11 M CH_3COOH solution. For example, Khanmirzaei et al. (2013) observed that the HCO_3^- anion was the main Cd complexing in the soil solution (slightly alkaline pH values), and that the dominant species in solution were Cd^{2+} and $CdHCO^+_3$, deducing that $CdCO_3$ can control Cd^{2+} concentration in solution.

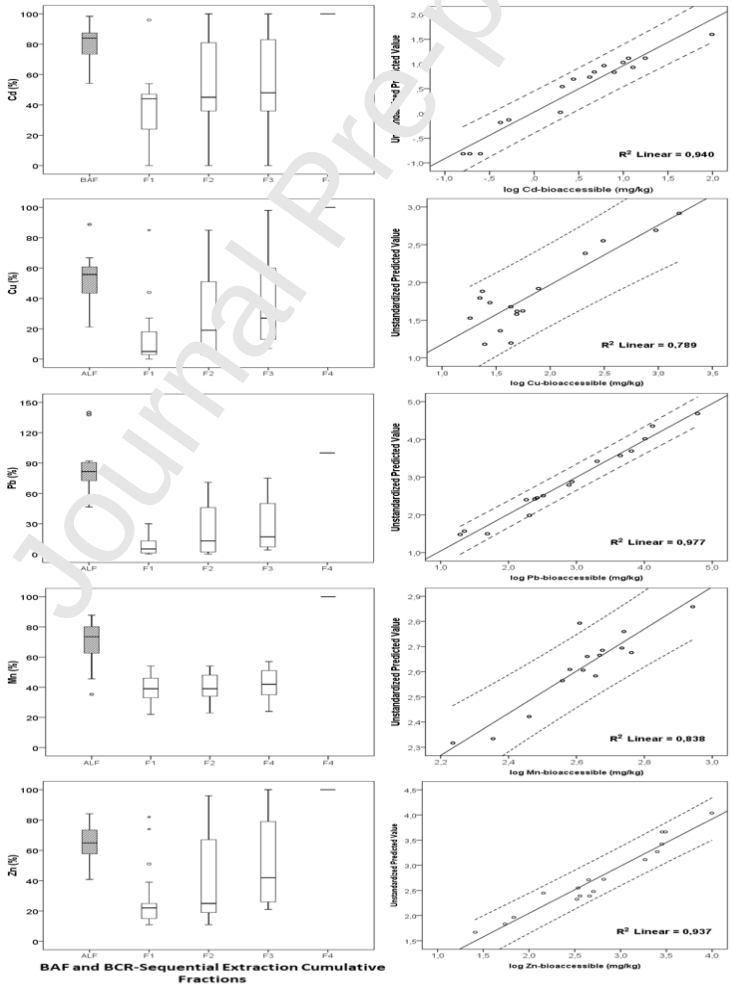

Figure 4. Cumulative solid-phase distribution and bioaccessible fraction (%) of potentially harmful elements in samples of urban matrices (10 µm). BAF— bioaccessible fraction (%). F1: Exchangeable and acid soluble carbonate fraction; F2: hydroxides and mixed oxy-hydroxide phases (reducible fraction); F3: Organic substance

and sulphide fraction (oxidizable fraction) and; F4: the residual non-silicate bound trace metal concentration (Left side). Scatterplots of bioaccessible concentration (mg kg $^{-1}$) versus bioaccessible concentrations predicted by the regression model (Right side).

Samples from Apiaí (1AP, 2AP, 3AP and 4AP) had Zn concentrations in F1 ranging from 39 to 84% (2,830 to 9,920 mg kg^{-1}) of the pseudo-total concentration resulting in the accumulation of Zn in the surface of matrix. The relative abundance of Zn in the solid fractions in tailing samples decreased in the order of F1 > F4 > F2 > F3. These results were similar with those found by Kasemodel et al. (2019) in soil samples from a former Pb slag deposit and in a Pb beneficiation Plant at Adrianópolis, state of Paraná, southern of Brazil.

In the sediment samples, 43 and 48% of Cd and Mn (median values), respectively are associated with the F1. The F1 fraction of Cd varied from 0 to 49% in the soil samples, 23 to 84% in the tailing matrix, and 38 to 48% in sediments. In soils, a higher proportion of Mn was found in F1 (median = 40%), though a soil sample (58PC) had almost 85% of the total content in the F1 (Figure 4G). Hernández-Pellón et al. (2019) observed that Mn compounds in the water-soluble fraction were highest than the other fractions in PM_{10} samples from an urban area impacted by a Mn alloy plant. This may be because of Mn oxide reaction with NO_2, SO_2 and HCl gases from atmosphere pollution found in industrial areas, producing soluble salts, i.e., $MnSO_4$, $Mn(NO_3)_2$, $Mn(NO_3)_2$, $MnCl_2$. The water-soluble fraction is assumed to be part of F1 in the BCR-sequential extraction.

Three soil samples, two collected in the city of Piracicaba (35PC and 47PC), and one collected in a native forest in the city of Apiaí (5AP) had the concentration of Cd extracted by the 0.11 mol L^{-1} acetic acid (Rauret et al., 1999) lower than the LQ (0.005 mg L^{-1}). However, Cd was associated with either the F2, reducible fraction (47PC = 99% and 5AP = 83%) or the F4, residual fraction (35PC = 100%). Colzato et al. (2017) observed similar result in a Brazilian Typic Argiudoll which had 75% of Cd extracted by 0.5 mol L^{-1} $NH_2OH.HCl$.

A larger proportion of Pb and Cu (n = 17, median = 5%, percentile 25th: 1.2 and 2.5 %; percentile 75th: 13.4 and 18.7 %, respectively) were present in F1 compared to the other elements (Figure 4 C and E). This is most likely to be due to a pH > 6 that favoured the formation of precipitates or insoluble substances and to the presence of organic matter, since organic carbon ranged from 0.5 to 6.5% (Table 2), thus forming stable complexes with PHE. Conversely, Witt III et al. (2014) evaluated Pb dust collected in a mining area and observed that the high proportion of Pb in the mobile fraction was associated with the presence of cerussite ($PbCO_3$), litharge (PbO) and anglesite ($PbSO_4$) that are soluble in acetic acid solution. However, in this study,

the highest proportion of Pb was found in F4 (residual) with median 89% for sediment, 86% for soils and 51% for tailing. In general, soil Pb is immobile at high pH and when associated with silicate fraction (Shotyk and Le Roux, 2005).

In the F2 fraction (reducible phase) the behaviour of the elements is site-specific, i.e. soil samples 47PC, 5AP and 9SA showed Cd, Cu, Pb, Mn and Zn associated with this fraction, but this was not shown in the other samples. The same behaviour was also observed in sediment 8SA and tailings samples 2AP, 3AP and 4AP. Tailing samples had higher concentrations of Cd, Cu, Pb and Mn in F2 compared to the sediment and soil samples, indicating that these elements may be bound to Fe/Mn oxides. A high median content was observed for Cu and Pb (> 30%) in tailing samples 2AP, 3AP and 4AP, compared to Cd, Mn and Zn. Samples 1AP and 1SA did not have levels available in this fraction (Figure S4).

In the samples not mentioned here Cd, Cu, Pb and Mn concentrations were below the limit of quantification (0.01 mg L^{-1}) and some samples of sediments and soils had low concentrations of Zn on F2 (< 2 mg kg^{-1}). Generally, soils from humid tropical regions have a high degree of weathering, predominating minerals such as kaolinite and oxides/hydroxides of Fe and Al, such as hematite (Fe_2O_3), goethite (FeOOH) and gibbsite ($Al(OH)_3$) whose electrical charge are highly pH dependent (Fontes and Alleoni, 2006). Therefore, extraction with 0.11 mol L^{-1} CH_3COOH (pH ≈ 2.9, pKa 4.76) may have formed positive charges by the adsorption of H^+ on the edge surface causing the destabilization of the variable charges minerals releasing the metals to the extraction solution (F1) thereby, the F2 may have been underestimated. Therefore, samples that may contain high content of hematite or goethite were not fully solubilized, which prevented the release of oxide-occluded metals to solution.

The hydroxylamine hydrochloride reagent used in the F2 extraction can moderately dissolve Fe oxides/hydroxides in soils or sediments; however Mn solubility is more significant, as shown by Chao (1972), who evaluated the dissolution of Fe and Mn oxides in samples of soils and sediments with acidified hydroxylamine hydrochloride. Chao (1972) observed that 50% of Mn and 1% of Fe from highly weathered soils were solubilized and the major part of iron oxides remained in the residue. F3 is related to the oxidizable fraction of a test material, that is, the fraction of the elements linked to organic matter or to sulphides (Rauret et al., 1999). There was little expression of this fraction in all samples studied, with relative amounts < 17%.

The Kruskal-Wallis test showed that there were no differences in the distribution of Cu ($H(2) = 5.809$, $p = 0.055$) and Mn ($H(2)$; $p = 0.277$) values in the F3 and that for Cd ($p = 0.041$), Pb ($p = 0.020$) and Zn ($p = 0.002$) there were differences in the distribution of data. The relative abundance of PHE in the different urban

matrices found in F3 decreases as follows: Cd in sediments (7%) > tailings (5%) > soils (1%), Cu in soil (12%) > sediment (9%) > tailings (7%), Pb in soil (5%) ≈ sediment (4%) ≈ tailing (3%), Zn in soil (3%) ≈ sediment (3%) > tailing (1%) and soil (12%) > sediment (9%) > tailing (6%)

When the two first fractions were examined together (sum of F1 (exchangeable and acid soluble carbonate) + F2 (hydroxides and mixed oxy-hydroxide phases (reducible fraction))), the most mobilizable elements were Cd (46%) and Mn (40%) in soils, Cd (43%) and Mn (50%) in sediments, and Zn (82%) > Cd (61%) > Cu (54%) > Pb (45%) > Mn (40%) in tailings. The samples containing considerable proportions of PHE in the mobile and reducible phases were likely to be derived from anthropogenic sources, while the less mobile (oxidizable and residual) were linked to geogenic sources (Borgese et al., 2013; Patinha et al., 2015).

The soil samples were collected in urban regions of the Piracicaba city (Table 1) which is in one of the main industrial centres of the interior region of the state of São Paulo. Cd, Cu and Zn are generally derived from industries, vehicle traffic, exhaust fumes and atmospheric deposition (Shi et al., 2013) and can be found in considerable proportions in urban soils. On the other hand, sediment and soil samples collected in Santo Amaro (Table 1), which is a smaller and less industrialized city than Piracicaba, may have had the contribution of the tailing used as streets paving, as well as domestic waste improperly deposited on the streets.

A high percentage of all elements (> 50%) are associated with residual fraction (F4) for all matrices, i.e. these elements may be either related to the silicate matrix of the samples or present in several metal alloys not dissolved by the reagent solutions used in the previous fractions. On the other hand, a low proportion of Cd was found in samples 47PC (5%) with no significant amount in samples of soil (9SA) and tailings (3AP), as can be seen in Figure S4 (Supplementary material); 2% of Cu in soil sample 58PC, 4% of Zn in sample 8SA (sediment) and no significant amounts in the tailing samples 3AP and 4AP (Figure S4). These samples (with low Cd and Cu amounts in the residual fraction) had the highest proportions of the PHE referenced, associated to F2, which could be bound to the Mn oxides, but the pseudo-total concentration of Fe was higher than that of Mn (48 to 118 times) suggesting that Fe may be controlling the mobility of the elements at this fraction.

3.3.2 Identification of the sources of PHE bioaccessibility using BCR-sequential extraction and MLR

When comparing results of the respiratory bioaccessibility extraction with the sequential extraction, it was observed that the simulated fluid could extract all the solid phases in most of the samples (Figure S4), including some of the residual phase. It means that it was able to extract those elements strongly adsorbed to the crystalline phase of the matrix.

The chemical fractionation of urban environmental matrices provided the estimate of bioaccessibility of Cd, Cu, Mn, Pb and Zn. The determination coefficients (R^2) ranged from 0.79 to 0.98 and in the SLF. The MLR allowed identification of the main geochemical sources as significant predictors of the respiratory bioaccessibility. The adjusted final models are shown in Table 3. The MLR presented both F1 (soluble and exchangeable phase) and F3 (oxidizable fraction) as the main predictors for Cd bioaccessibility. Both fractions contributed with same impact in the model (b_{F1} = 0.34 and b_{F3} = 0.32, R^2 = 0.94, $p < 0.001$). The ALF fluid (pH 4.5) dissolved Cd in all solid fractions (Figures 4A and 4B) in the matrices; however, the impact of Cd bound to the exchangeable/carbonate and oxidizable forms was stronger than the reducible and residual forms. Metals bound to the exchangeable and carbonated phases can easily become mobile and available under low pH conditions, and thereby potentially harmful to human health. Metals such Cd can produce reactive oxygen species (ROS) able to cause inflammatory diseases in the lungs (Julien et al., 2011).

Table 3 Model for prediction of respiratory bioaccessibility of Cd, Cu, Pb, Mn and Zn from urban environmental matrices

Element	Equation model**	R^2	S.E.*
Cd	$\log Cd_{ALF} = 0.82 + 0.34 \log Cd_{F1} + 0.32 \log Cd_{F3}$	0.94	0.21
Cu	$\log Cu_{ALF} = 0.76 + 0.94 \log Cu_{F3}$	0.79	0.28
Pb	$\log Pb_{ALF} = 0.012 + 1.24 \log Pb_{F4} + .082 \log Pb_{F2}$	0.98	0.17
Mn	$\log Mn_{ALF} = -0.55 + 1.03 \log Mn_{F1} + 0.29 \log Mn_{F4}$	0.84	0.07
Zn	$\log ZnALF = 0.27 + 0.81 \log Zn_{F1}$	0.94	0.18

* Standard error of estimate

** *p < 0.001*

The predicted model for Cu bioaccessibility (Figure 4D) only had F3 (the oxidizable fraction) as the main factor that affected the bioaccessibility (R^2 = 0.8). This factor was already expected since Cu has high affinity to organic complexes that can be associated with the oxidizable fraction (Yang et al., 2018). In the presence of organic anions, Cd and Cu behaviours in the soil can be altered. The presence of acetate may increase the amount of Cu associated with the organic matter, as well as in the presence of citrate, Cu linked to carbonate and occluded in manganese oxides is less pronounced (Ahumada et al., 2001).

In the case of Pb, 98% of respiratory bioaccessibility can be explained by the covariates, F4 and F2 in

this model (Figure 4F). The impact of F4 (residual fraction) is greater than F2 (reducible), it can be verified by the magnitude of the *t* statistic test ($t_{F4}(13) = 22.8$; $t_{F2}(13) = 5.2$). Pb bioaccessibility is highly dependent of mineralogical composition and weathered conditions as well as to the phosphate present in the ALF fluid. The presence of phosphate may limit the Pb solubility because of formation of low-soluble substances, such as pyromorphite ($Pb_5Cl(PO_4)_3$), even in environments with low pH values (Schaider et al., 2007). In our study, however, in which the bioaccessibility of Pb ranged from 46 to 140% of the pseudo-total content, it is possible that there were Pb species with greater lability, such as halides and carbonates forms, Pb oxides or adsorbed on surface of Fe and Mn hydroxide (Rieuwerts et al., 2000).

F1 (exchangeable/carbonates) and F4 (residual) were the predictive variables for Mn-bioaccessibility with the fitted model explaining 80% of the variation (Figure 4H). The effect of F1 was higher than F4 ($t_{F1}(12) = 1.0$; $t_{F4}(12) = 0.3$). Mn bioaccessible varied from 35 to 88% and Mn-F1 varied from 22 to 54%. Similar bioaccessibility fraction (52%) and labile fraction of Mn (71%) was found by (Voutsa and Samara, 2002) at urban and industrial sites suggesting the predominance of soluble forms in urban atmospheric particles.

The MLR identified F1 as the only predictor of Zn bioaccessibility ($R^2 = 0.94$) (Figure 4J). The positive correlation between Zn-ALF and Zn-F1 suggest that the Zn species are likely derived from poorly crystalline secondary mineral forms easily soluble in soil solution (Molina et al., 2013). Molina et al. (2013) observed that there was a higher Zn bioavailability and bioaccessibility in mine waste at pH 1.5 and 4.5 than at pH 7.4; and *in vitro* bioaccessibility decreased as follows: mine waste > hydrozincite > hemimorphite > zincite ≈ smithsonite >> sphalerite, where the first three materials contained more than 81% of Zn in the labile phase (exchangeable ions and carbonates) and demonstrated that the mineralogy was the main factor that contributes to the bioaccessibility.

4. Conclusions

The Brazilian Resolution, CONAMA #420, recommends the use of strong acid solutions to extract inorganic substances for soils sieved with a 2 mm mesh, but the use of these procedures to extract the contents of PHE and the particle size do not necessarily estimate the respiratory bioaccessibility. Therefore, a more detailed analysis from each contaminated site and adequate sample preparation is required. It is recommended that the extraction be performed on particles with less than 10 μm to simulate the size fraction that can reach the respiratory tract.

Mn bioaccessibility may have been influenced by mineralogy, especially in sediment samples, where there was a predominance of 2: 1 minerals and kaolinite. Although Mn is not included in the Brazilian soil

quality guideline, the results of this study show that 35 to 88% of the pseudo-total Mn concentration is bioaccessible, which suggests that this PHE requires further attention, mainly in a HHRA. In addition, the mine tailings samples contained the highest pseudo-total concentrations of PHE in comparison to the soil and sediment samples, both in the bulk soil and fine fraction. However, all three matrices contained more than 60% of bioaccessible PHE contents. These results lead us to highlight the importance of including the *in vitro* method of respiratory bioaccessibility to provide a more realistic estimate of PHE concentrations in UEM that are potentially available to humans.

MRL models were useful to differentiate the main solid fractions that influence the PHE bioaccessibility, and the variation in the respiratory bioaccessibility of PHE should be attributed to differences in both chemical and mineralogical characteristics of the matrices.

More detailed investigation into contaminated areas can serve as a basis for determining the physicochemical characteristics of inhalable/respirable particulate materials, in addition to assessing possible adverse effects on the environment and human health.

This study may serve as a basis for toxicological studies and for the development of new strategies for evaluating sites considered contaminated. The different PHE do not necessarily have the same behaviour in different matrices. So, each case must be carefully investigated. The development of public policies by stakeholders should consider the bioaccessibility results as one of the evaluation criteria in the HHRA for each contaminated site, as well as the geochemical behaviour of each PHE so that there is adequate information to support a good estimate based on risk associated with the environmental matrix.

Acknowledgments

This study was supported by the São Paulo Research Foundation (FAPESP) [grants # 15/19332-9 and # 15/24483-9]; by the Brazilian National Council for Scientific and Technological Development (CNPq) [grant # 404164/2016]. The authors thank the Department of Geoscience, University of Aveiro, Portugal, for their support in the development of the laboratory work. Dr Marina Colzato at ESALQ is gratefully acknowledged for performing the ICP-OES analyses. The authors also acknowledge the assistance and support provided by the Centre for Research in Geochemistry and Geophysics of the Lithosphere (NUPEGEL-USP) in the mineralogical analyses.

CRediT authorship contribution statement

A.B.: Conceptualization, Investigation, Formal analysis, Data curation, Writing - Original Draft, Writing - review & editing and Funding acquisition. **C.P.:** Validation, Investigation, Resources and Writing - review &

editing. **J.W.:** Conceptualization, Validation, Formal analysis and Writing - review & editing. **M.C.:** Formal analysis and Writing - review & editing. **L.A.:** Conceptualization, Resources, Supervision, Funding acquisition and Writing - review & editing

References

Abdu, N., Agbenin, J.O., Buerkert, A., 2012. Fractionation and mobility of cadmium and zinc in urban vegetable gardens of Kano, Northern Nigeria. Environ. Monit. Assess. 184, 2057–2066. https://doi.org/10.1007/s10661-011-2099-2

Ahumada, I., Mendoza, J., Escudero, P., Ascar, L., 2001. Effect of acetate, citrate, and lactate incorporation on distribution of cadmium and copper chemical forms in soil. Commun. Soil Sci. Plant Anal. 32, 771–785. https://doi.org/10.1081/CSS-100103908

Batista, A.H., Melo, V.F., Gilkes, R., Roberts, M., 2018. Identification of heavy metals in crystals of sand and silt fractions of soils by scanning electron microscopy (SEM EDS/WD-EPMA). Rev. Bras. Cienc. do Solo 42. https://doi.org/10.1590/18069657rbcs20170174

Boisa, N., Elom, N., Dean, J.R., Deary, M.E., Bird, G., Entwistle, J.A., 2014. Development and application of an inhalation bioaccessibility method (IBM) for lead in the PM10 size fraction of soil. Environ. Int. 70, 132–142. https://doi.org/10.1016/j.envint.2014.05.021

Borgese, L., Federici, S., Zacco, A., Gianoncelli, A., Rizzo, L., Smith, D.R., Donna, F., Lucchini, R., Depero, L.E., Bontempi, E., 2013. Metal fractionation in soils and assessment of environmental contamination in Vallecamonica, Italy. Environ. Sci. Pollut. Res. 20, 5067–5075. https://doi.org/10.1007/s11356-013-1473-8

Calas, A., Uzu, G., Martins, J.M.F., Voisin, Di., Spadini, L., Lacroix, T., Jaffrezo, J.L., 2017. The importance of simulated lung fluid (SLF) extractions for a more relevant evaluation of the oxidative potential of particulate matter. Sci. Rep. 7. https://doi.org/10.1038/s41598-017-11979-3

Carvalho, F.M., 2013. Mapa do solo contaminado por elementos químicos em Santo Amaro da Purificação, in: I Simpósio de Atualização Científica (SACSA). UFBA, Santo Amaro.

Cave, M., 2012. Bioaccessibility of potentially harmful soil elements. Environ. Sci. 21, 26–29.

CETEM – Centre for Mineral Technology, 2012. Santo Amaro (BA) coexists with socio-environmental liabilities of former metallurgical industry. CETEM - Banco dados verbetes 4.

Chao, T.T., 1972. Selective Dissolution of Manganese Oxides from Soils and Sediments with Acidified Hydroxylamine Hydrochloride. Soil Sci. Soc. Am. J. 36, 764–768.

https://doi.org/10.2136/sssaj1972.03615995003600050024x

Colombo, C., Monhemius, A.J., Plant, J.A., 2008. Platinum, palladium and rhodium release from vehicle exhaust catalysts and road dust exposed to simulated lung fluids. Ecotoxicol. Environ. Saf. 71, 722–730. https://doi.org/10.1016/j.ecoenv.2007.11.011

Colzato, M., Kamogawa, M.Y., Carvalho, H.W.P., Alleoni, L.R.F., Hesterberg, D., 2017. Temporal Changes in Cadmium Speciation in Brazilian Soils Evaluated Using Cd L III -Edge XANES and Chemical Fractionation. J. Environ. Qual. 46, 1206–1214. https://doi.org/10.2134/jeq2016.08.0316

CONAMA, – National Environment Council, 2012. RESOLUTION No. 420, December 28, 2009 Published in Official Gazette 249 on 12/30/2009, pp. 81-84, in: Current Conama Resolutions Published between September 1984 and January 2012. Ministry of the Environment (MMA), Brasília, DF, Brazil, pp. 748–762.

Cruz, N., Rodrigues, S.M., Tavares, D., Monteiro, R.J.R.R., Carvalho, L., Trindade, T., Duarte, A.C., Pereira, E., Römkens, P.F.A.M.A.M., 2015. Testing single extraction methods and in vitro tests to assess the geochemical reactivity and human bioaccessibility of silver in urban soils amended with silver nanoparticles. Chemosphere 135, 304–311. https://doi.org/10.1016/j.chemosphere.2015.04.071

de Andrade Lima, L.R.P.P., Bernardez, L.A., 2011. Characterization of the lead smelter slag in Santo Amaro, Bahia, Brazil. J. Hazard. Mater. 189, 692–699. https://doi.org/10.1016/j.jhazmat.2011.02.091

de Andrade, M.F., Moraes, L.R.S., 2013. Lead contamination in Santo Amaro defies decades of research and delayed reaction on the part of the public authorities. Ambient. e Soc. 16, 63–80. https://doi.org/10.1590/S1414-753X2013000200005

Dias, C.L., Lemos, M.M.G., Casarini, D.C.P., Ohba, M.S., de Oliveira Filha, M.T., 2006. Valores Orientadores de intervenção e sua aplicação no gerenciamento de áreas contaminadas, in: XIV Congresso Brasileiro de Águas Subterrâneas. Associação Brasileira de Águas Subterrâneas - ABAS, São Paulo, pp. 1–18.

Dieter, H.H., Bayer, T.A., Multhaup, G., 2005. Environmental copper and manganese in the pathophysiology of neurologic diseases (Alzheimer's disease and manganism). Acta Hydrochim. Hydrobiol. 33, 72–78. https://doi.org/10.1002/aheh.200400556

Dixon, J.., Weed, S.., 1989. Minerals in soil environments, 2sd ed. Soil Science Society of America, Madison, Wisconsin, USA.

Donagema, G.K., Campos, D.V.B. de, Calderano, S.B., Teixeira, W.G., Viana, J.H.M., 2011. Manual de método e análise de solo, 2nd ed. Embrapa Solos, Rio de Janeiro.

Drysdale, M., Ljung Bjorklund, K., Jamieson, H.E.H.E., Weinstein, P., Cook, A., Watkins, R.T., Bjorklund, K.L., Jamieson, H.E.H.E., Weinstein, P., Cook, A., Watkins, R.T., 2012. Evaluating the respiratory bioaccessibility of nickel in soil through the use of a simulated lung fluid. Environ. Geochem. Health 34, 279–288. https://doi.org/10.1007/s10653-011-9435-x

FAO – Food and Agriculture Organization of the United Nations, 2014. World reference base for soil resources 2014. International soil classification system for naming soils and creating legends for soil maps, World Soil Resources Reports No. 106.

Fontes, M.M.P.F., Alleoni, L.R.F.L., 2006. Electrochemical attributes and availability of nutrients, toxic elements, and heavy metals in tropical soils. Sci. Agric. 63, 589–608. https://doi.org/10.1590/s0103-90162006000600014

Galle, P., Berry, J.P., Galle, C., 1992. Role of alveolar macrophages in precipitation of mineral elements inhaled as soluble aerosols. Environ. Health Perspect. 97, 145–147. https://doi.org/10.1289/ehp.9297145

Gilkes, R.J., McKenzie, R.M., 1988. Geochemistry and Mineralogy of Manganese in Soils, in: Manganese in Soils and Plants. pp. 23–35. https://doi.org/10.1007/978-94-009-2817-6_3

Guney, M., Bourges, C.M.-J.M.J., Chapuis, R.P., Zagury, G.J., 2017. Lung bioaccessibility of As, Cu, Fe, Mn, Ni, Pb, and Zn in fine fraction (< 20 μm) from contaminated soils and mine tailings. Sci. Total Environ. 579, 378–386. https://doi.org/10.1016/j.scitotenv.2016.11.086

Hedberg, Y., Hedberg, J., Liu, Y., Wallinder, I.O., 2011. Complexation- and ligand-induced metal release from 316L particles: Importance of particle size and crystallographic structure. BioMetals 24, 1099–1114. https://doi.org/10.1007/s10534-011-9469-7

Hedberg, Y.S., Odnevall Wallinder, I., 2016. Metal release from stainless steel in biological environments: A review. Biointerphases 11, 018901. https://doi.org/10.1116/1.4934628

Henderson, R.G., Verougstraete, V., Anderson, K., Arbildua, J.J., Brock, T.O., Brouwers, T., Cappellini, D., Delbeke, K., Herting, G., Hixon, G., Odnevall Wallinder, I., Rodriguez, P.H., Van Assche, F., Wilrich, P., Oller, A.R., 2014. Inter-laboratory validation of bioaccessibility testing for metals. Regul. Toxicol. Pharmacol. 70, 170–181. https://doi.org/10.1016/j.yrtph.2014.06.021

Hernández-Pellón, A., Mazón, P., Fernández-Olmo, I., 2019. Quantification of manganese species in particulate matter collected in an urban area nearby a manganese alloy plant. Atmos. Environ. 205, 46–51. https://doi.org/10.1016/j.atmosenv.2019.02.040

Hernández-Pellón, A., Nischkauer, W., Limbeck, A., Fernández-Olmo, I., 2018. Metal(loid) bioaccessibility and

inhalation risk assessment: A comparison between an urban and an industrial area. Environ. Res. 165, 140–149. https://doi.org/10.1016/j.envres.2018.04.014

Hooda, P.S., 2010. Trace Elements in Soils. Wiley. https://doi.org/10.1002/9781444319477

Huang, M., Chen, X., Zhao, Y., Yu Chan, C., Wang, W., Wang, X., Wong, M.H., 2014. Arsenic speciation in total contents and bioaccessible fractions in atmospheric particles related to human intakes. Environ. Pollut. 188, 37–44. https://doi.org/10.1016/j.envpol.2014.01.001

Julien, C., Esperanza, P., Bruno, M., Alleman, L.Y., 2011. Development of an in vitro method to estimate lung bioaccessibility of metals from atmospheric particles. J. Environ. Monit. 13, 621. https://doi.org/10.1039/c0em00439a

Kasemodel, M.C., Papa, T.B.R., Sígolo, J.B., Rodrigues, V.G.S., 2019. Assessment of the mobility, bioaccessibility, and ecological risk of Pb and Zn on a dirt road located in a former mining area—Ribeira Valley—Brazil. Environ. Monit. Assess. 191, 1–15. https://doi.org/10.1007/s10661-019-7238-1

Kastury, F., Smith, E., Juhasz, A.L., 2017. A critical review of approaches and limitations of inhalation bioavailability and bioaccessibility of metal(loid)s from ambient particulate matter or dust. Sci. Total Environ. 574, 1054–1074. https://doi.org/10.1016/j.scitotenv.2016.09.056

Khanmirzaei, A., Bazargan, K., Amir Moeezi, A., Richards, B.K., Shahbazi, K., 2013. Single and sequential extraction of cadmium in some highly calcareous soils of Southwestern Iran. J. Soil Sci. Plant Nutr. 13, 153–164. https://doi.org/10.4067/s0718-95162013005000014

Kim, J.O., Lee, Y.W., Chung, J., 2013. The role of organic acids in the mobilization of heavy metals from soil. KSCE J. Civ. Eng. 17, 1596–1602. https://doi.org/10.1007/s12205-013-0323-z

Kreyling, W.G., 1992. Intracellular particle dissolution in alveolar macrophages. Environ. Health Perspect. 97, 121–126. https://doi.org/10.1289/ehp.9297121

Kwakye, G., Paoliello, M., Mukhopadhyay, S., Bowman, A., Aschner, M., 2015. Manganese-Induced Parkinsonism and Parkinson's Disease: Shared and Distinguishable Features. Int. J. Environ. Res. Public Health 12, 7519–7540. https://doi.org/10.3390/ijerph120707519

Lamb, D.T., Ming, H., Megharaj, M., Naidu, R., 2009. Heavy metal (Cu, Zn, Cd and Pb) partitioning and bioaccessibility in uncontaminated and long-term contaminated soils. J. Hazard. Mater. 171, 1150–1158. https://doi.org/10.1016/j.jhazmat.2009.06.124

Leelasakultum, K., Kim Oanh, N.T., 2017. Mapping exposure to particulate pollution during severe haze episode using improved MODIS AOT-PM 10 regression model with synoptic meteorology classification.

GeoHealth 1, 165–179. https://doi.org/10.1002/2017gh000059

Lehnert, B.E., 1990. Alveolar Macrophages in a Particle "Overload" Condition. J. Aerosol Med. 3, S-9-S-30. https://doi.org/10.1089/jam.1990.3.Suppl_1.S-9

Ljung, K., Siah, W.S., Devine, B., Maley, F., Wensinger, A., Cook, A., Smirk, M., 2011. Extracting dust from soil: Improved efficiency of a previously published process. Sci. Total Environ. 410–411, 269–270. https://doi.org/10.1016/j.scitotenv.2011.07.061

Ljung, K., Torin, A., Smirk, M., Maley, F., Cook, A., Weinstein, P., 2008. Extracting dust from soil: A simple solution to a tricky task. Sci. Total Environ. 407, 589–593. https://doi.org/10.1016/j.scitotenv.2008.09.007

Lu, Z.B., Kang, M., 2018. Risk assessment of toxic metals in marine sediments from the Arctic Ocean using a modified BCR sequential extraction procedure. J. Environ. Sci. Heal. - Part A Toxic/Hazardous Subst. Environ. Eng. 53, 278–293. https://doi.org/10.1080/10934529.2017.1397443

Luo, X.S., Yu, S., Li, X.D., 2011. Distribution, availability, and sources of trace metals in different particle size fractions of urban soils in Hong Kong: Implications for assessing the risk to human health. Environ. Pollut. 159, 1317–1326. https://doi.org/10.1016/j.envpol.2011.01.013

Marôco, J., 2011. Análise estatística com o SPSS Statistics, 5th ed. Pero Pinheiro, Lisbon.

Marques, M.R.C., Loebenberg, R., Almukainzi, M., 2011. Simulated biologic fluids with possible application in dissolution testing. Dissolution Technol. 15–28. https://doi.org/10.1002/jps.23029

Martins, J., Figueiredo, B.R., 2014. Testes de mobilidade de chumbo e arsênio em solo contaminado em Apiaí (SP). Geochim. Bras. 28, 189–200. https://doi.org/10.5327/Z0102-9800201400020007

Molina, R.M., Schaider, L.A., Donaghey, T.C., Shine, J.P., Brain, J.D., 2013. Mineralogy affects geoavailability, bioaccessibility and bioavailability of zinc. Environ. Pollut. 182, 217–224. https://doi.org/10.1016/j.envpol.2013.07.013

Moreda-Piñeiro, J., Moreda-Piñeiro, A., Romarís-Hortas, V., Moscoso-Pérez, C., López-Mahía, P., Muniategui-Lorenzo, S., Bermejo-Barrera, P., Prada-Rodríguez, D., 2011. In-vivo and in-vitro testing to assess the bioaccessibility and the bioavailability of arsenic, selenium and mercury species in food samples. TrAC Trends Anal. Chem. 30, 324–345. https://doi.org/10.1016/j.trac.2010.09.008

Niu, J., Rasmussen, P.E., Hassan, N.M., Vincent, R., 2010. Concentration distribution and bioaccessibility of trace elements in nano and fine urban airborne particulate matter: Influence of particle size. Water. Air. Soil Pollut. 213, 211–225. https://doi.org/10.1007/s11270-010-0379-z

Oberdörster, G., Oberdörster, E., Oberdörster, J., 2005. Nanotoxicology: An Emerging Discipline Evolving from Studies of Ultrafine Particles. Environ. Health Perspect. 113, 823–839. https://doi.org/10.1289/ehp.7339

Patinha, C., Durães, N., Sousa, P., Dias, A.C., Reis, A.P., Noack, Y., Ferreira da Silva, E., 2015. Assessment of the influence of traffic-related particles in urban dust using sequential selective extraction and oral bioaccessibility tests. Environ. Geochem. Health 37, 707–724. https://doi.org/10.1007/s10653-015-9713-0

Pelfrêne, A., Cave, M.R., Wragg, J., Douay, F., 2017. In vitro investigations of human bioaccessibility from reference materials using simulated lung fluids. Int. J. Environ. Res. Public Health 14, 112. https://doi.org/10.3390/ijerph14020112

Puga, A.P., Melo, L.C.A., de Abreu, C.A., Coscione, A.R., Paz-Ferreiro, J., 2016. Leaching and fractionation of heavy metals in mining soils amended with biochar. Soil Tillage Res. 164, 25–33. https://doi.org/10.1016/j.still.2016.01.008

Ramos, M.E., Cappelli, C., Rozalén, M., Fiore, S., Huertas, F.J., 2011. Effect of lactate, glycine, and citrate on the kinetics of montmorillonite dissolution. Am. Mineral. 96, 768–780. https://doi.org/10.2138/am.2011.3694

Rauret, G., López-Sánchez, J.F., Sahuquillo, A., Rubio, R., Davidson, C., Ure, A., Quevauviller, P., 1999. Improvement of the BCR three step sequential extraction procedure prior to the certification of new sediment and soil reference materials. J. Environ. Monit. 1, 57–61. https://doi.org/10.1039/a807854h

Rieuwerts, J.S., Farago, M.E., Cikrt, M., Bencko, V., 2000. Differences in lead bioavailability between a smelting and a mining area. Water. Air. Soil Pollut. 122, 203–229. https://doi.org/10.1023/A:1005251527946

Santamaria, A.B., Sulsky, S.I., 2010. Risk Assessment of an Essential Element: Manganese. J. Toxicol. Environ. Heal. Part A 73, 128–155. https://doi.org/10.1080/15287390903337118

Schaider, L.A., Senn, D.B., Brabander, D.J., Mccarthy, K.D., Shine, J.P., 2007. Characterization of zinc, lead, and cadmium in mine waste: Implications for transport, exposure, and bioavailability. Environ. Sci. Technol. 41, 4164–4171. https://doi.org/10.1021/es0626943

Shi, X., Chen, L., Wang, J., 2013. Multivariate analysis of heavy metal pollution in street dusts of Xianyang city, NW China. Environ. Earth Sci. 69, 1973–1979. https://doi.org/10.1007/s12665-012-2032-1

Shotyk, W., Le Roux, G., 2005. Biogeochemistry and Cycling of Lead, in: Sigel, A., Siger, H., Siger, R.K. (Eds.), Metal Ions in Biological Systems. CRC Press, pp. 239–275.

https://doi.org/10.1201/9780824751999.ch10

Tong, Y., Yang, H., Tian, X., Wang, H., Zhou, T., Zhang, S., Yu, J., Zhang, T., Fan, D., Guo, X., Tabira, T., Kong, F., Chen, Z., Xiao, W., Chui, D., 2014. High Manganese, A Risk for Alzheimer's Disease: High Manganese Induces Amyloid-β Related Cognitive Impairment. J. Alzheimer's Dis. 42, 865–878. https://doi.org/10.3233/JAD-140534

Tronde, A., 2002. Pulmonary drug absorption: In vitro and in vivo investigations of drug absorption across the lung barrier and its relation to drug physicochemical properties. Uppsala University.

Unda-Calvo, J., Martínez-Santos, M., Ruiz-Romera, E., 2017. Chemical and physiological metal bioaccessibility assessment in surface bottom sediments from the Deba River urban catchment: Harmonization of PBET, TCLP and BCR sequential extraction methods. Ecotoxicol. Environ. Saf. 138, 260–270. https://doi.org/10.1016/j.ecoenv.2016.12.029

USEPA – United States Environmental Protection Agency, 2007. Method 3051A - Microwave assisted acid digestion of sediments, sludges, soils, and oils (rev. 3051A).

USEPA – United States Environmental Protection Agency, 1995. Integrated Risk Information System: Manganese; CASRN 7439-96-5.

Voutsa, D., Samara, C., 2002. Labile and bioaccessible fractions of heavy metals in the airborne particulate matter from urban and industrial areas. Atmos. Environ. 36, 3583–3590. https://doi.org/10.1016/S1352-2310(02)00282-0

Wei, M., Chen, J., Sun, Z., Lv, C., Cai, W., 2015. Distribution of Heavy Metals in Different Size Fractions of Agricultural Soils Closer to Mining Area and its Relationship to TOC and Eh, in: World Congress on New Technologies. Barcelona, pp. 1–6.

WHO – World Health Organization, 2000. Air quality guidelines for Europe, 2nd ed. WHO Regional Office for Europe, Copenhagen.

Wiseman, C.L.S., 2015. Analytical methods for assessing metal bioaccessibility in airborne particulate matter: A scoping review. Anal. Chim. Acta 877, 9–18. https://doi.org/10.1016/j.aca.2015.01.024

Witt, E.C., Shi, H., Wronkiewicz, D.J., Pavlowsky, R.T., 2014. Phase partitioning and bioaccessibility of Pb in suspended dust from unsurfaced roads in Missouri-A potential tool for determining mitigation response. Atmos. Environ. 88, 90–98. https://doi.org/10.1016/j.atmosenv.2014.02.002

Wragg, J., Klinck, B., 2007. The bioaccessibility of lead from Welsh mine waste using a respiratory uptake test. J. Environ. Sci. Heal. - Part A Toxic/Hazardous Subst. Environ. Eng. 42, 1223–1231.

https://doi.org/10.1080/10934520701436054

Yang, K., Zhang, T., Shao, Y., Tian, C., Cattle, S.R., Zhu, Y., Song, J., 2018. Fractionation, bioaccessibility, and risk assessment of heavy metals in the soil of an urban recreational area amended with composted sewage sludge. Int. J. Environ. Res. Public Health 15, 613. https://doi.org/10.3390/ijerph15040613

Zhao, S., Duan, Y., Lu, J.J., Gupta, R., Pudasainee, D., Liu, S., Liu, M., Lu, J.J., 2018. Chemical speciation and leaching characteristics of hazardous trace elements in coal and fly ash from coal-fired power plants. Fuel 232, 463–469. https://doi.org/10.1016/j.fuel.2018.05.135

Zhong, L., Yu, Y., Lian, H. zhen, Hu, X., Fu, H., Chen, Y. jun, 2017. Solubility of nano-sized metal oxides evaluated by using in vitro simulated lung and gastrointestinal fluids: implication for health risks. J. Nanoparticle Res. 19, 1–10. https://doi.org/10.1007/s11051-017-4064-7

Declaration of interests

☒ The authors declare that they have no known competing financial interests or personal relationships that could have appeared to influence the work reported in this paper.

☐The authors declare the following financial interests/personal relationships which may be considered as potential competing interests:

.

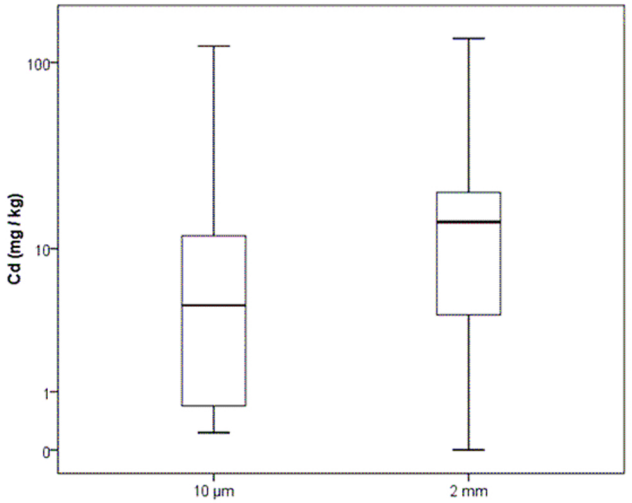
Cd (mg / kg)
100
10
1
0
10 µm
2 mm

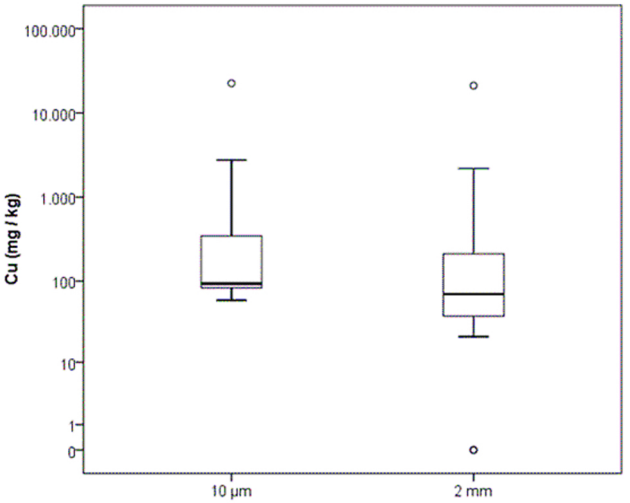
Cu (mg / kg)
100.000
10.000
1.000
100
10
1
0
10 µm
2 mm

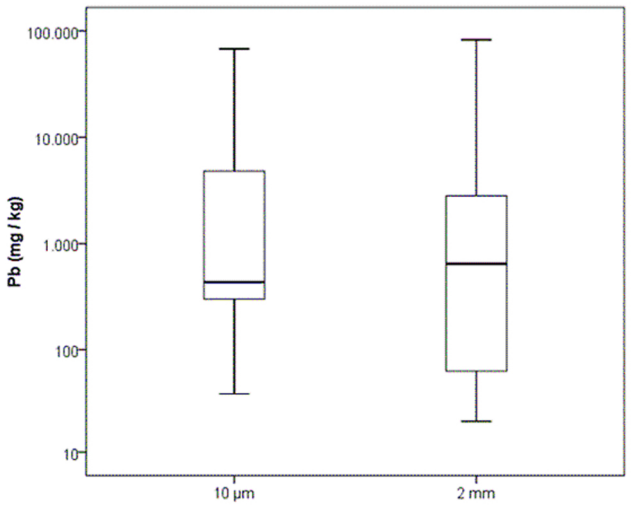
Pb (mg / kg)
100.000
10.000
1.000
100
10
10 µm
2 mm

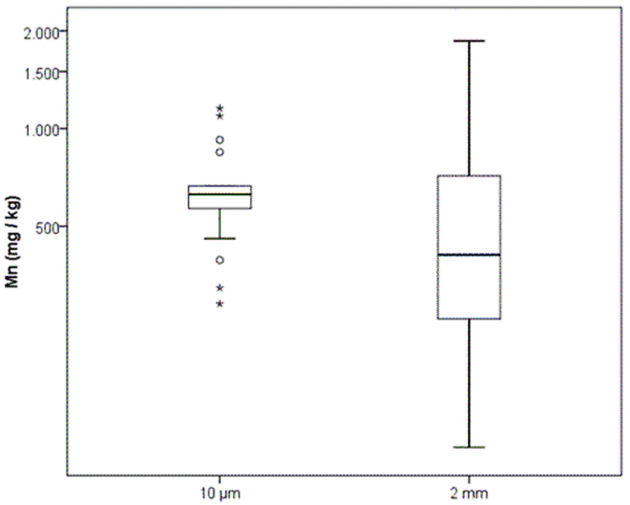
Mn (mg / kg)
2.000
1.500
1.000
500
10 µm
2 mm

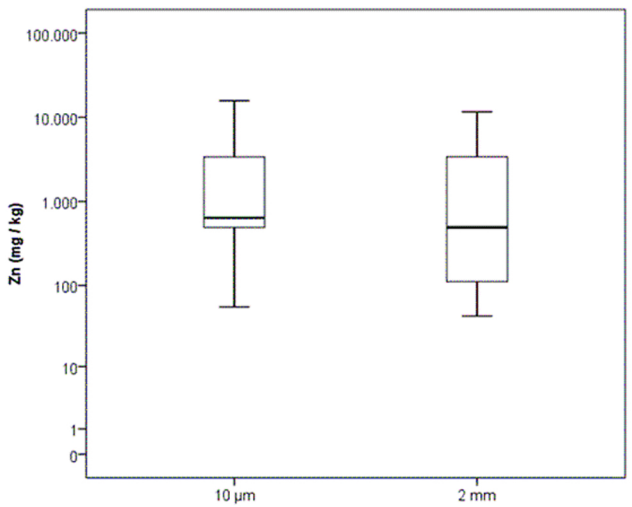
Zn (mg / kg)
100.000
10.000
1.000
100
10
1
0
10 µm
2 mm

Figure 1

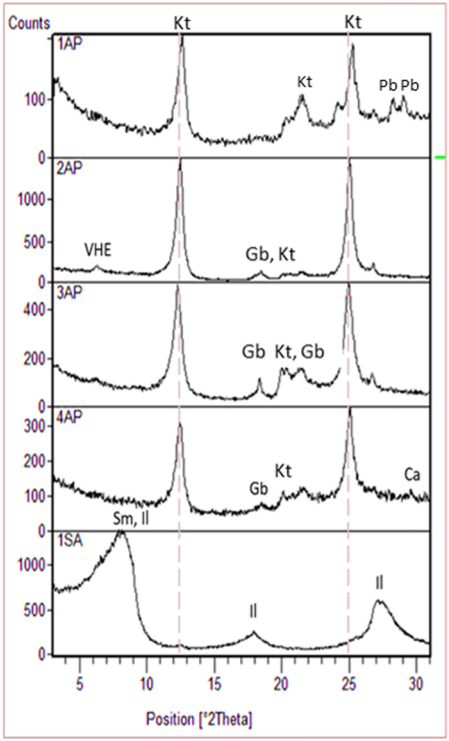

Tailing (a)

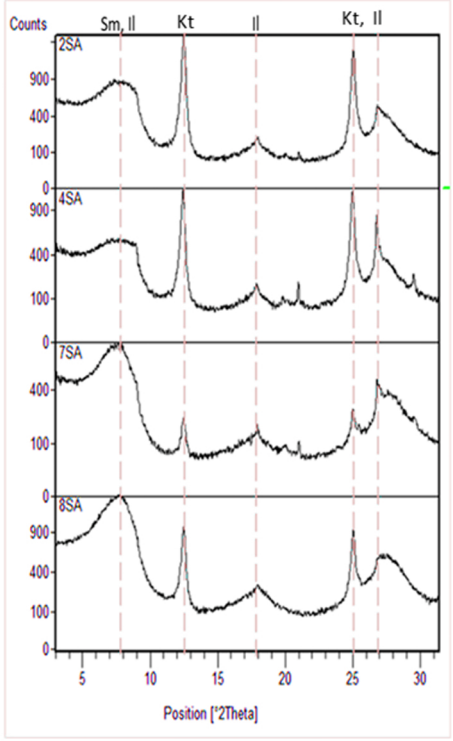

Sediment (b)

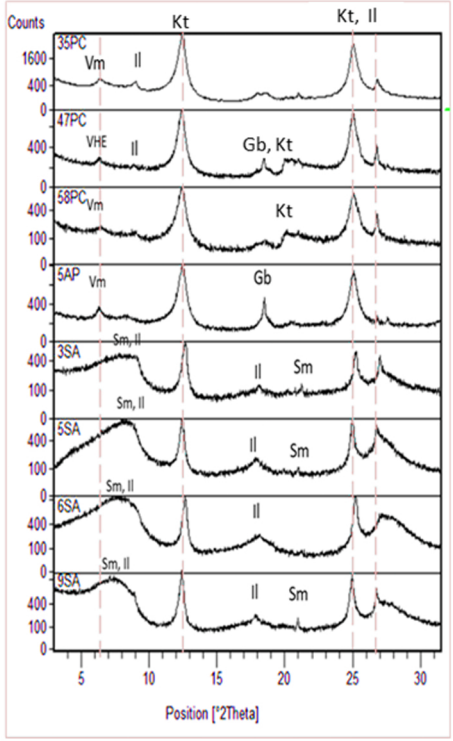

Soil (c)

Figure 2

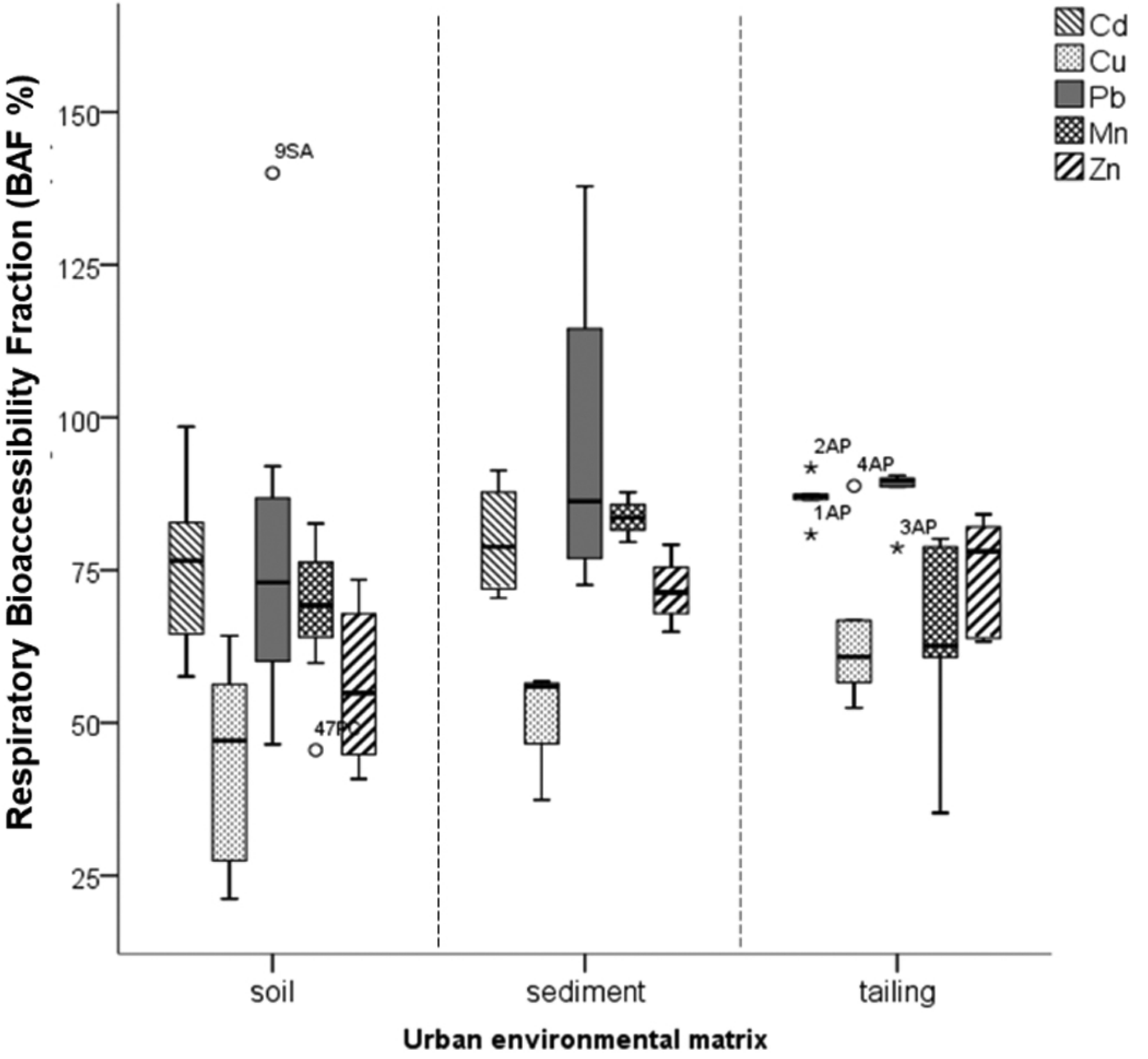
Cd
Cu
Pb
Mn
Zn
Respiratory Bioaccessibility Fraction (BAF %)
150
125
100
75
50
25
9SA
47PC
2AP
4AP
1AP
3AP
soil
sediment
tailing
Urban environmental matrix

Figure 3

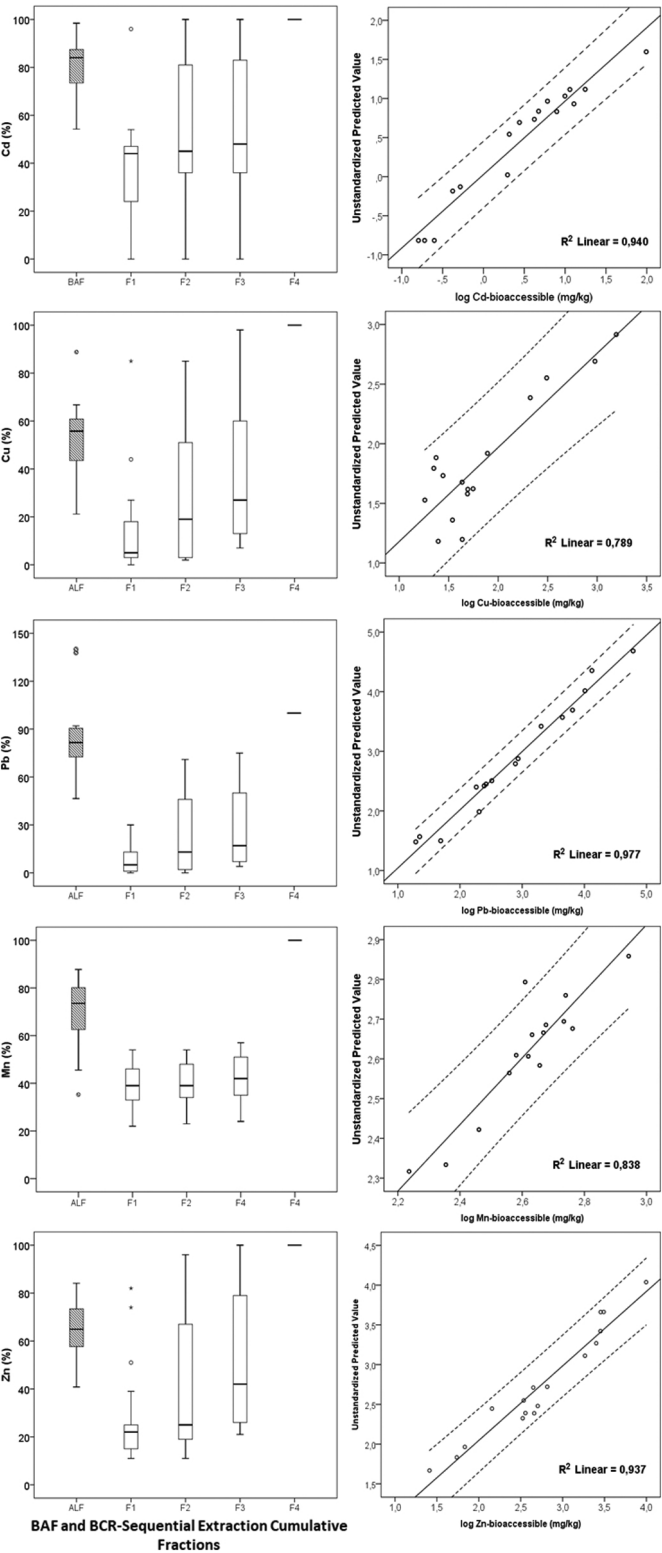
Cd (%)
BAF
F1
F2
F3
F4
Unstandardized Predicted Value
log Cd-bioaccessible (mg/kg)
R² Linear = 0,940
Cu (%)
ALF
F1
F2
F3
F4
Unstandardized Predicted Value
log Cu-bioaccessible (mg/kg)
R² Linear = 0,789
Pb (%)
ALF
F1
F2
F3
F4
Unstandardized Predicted Value
log Pb-bioaccessible (mg/kg)
R² Linear = 0,977
Mn (%)
ALF
F1
F2
F4
F4
Unstandardized Predicted Value
log Mn-bioaccessible (mg/kg)
R² Linear = 0,838
Zn (%)
ALF
F1
F2
F3
F4
Unstandardized Predicted Value
log Zn-bioaccessible (mg/kg)
R² Linear = 0,937
BAF and BCR-Sequential Extraction Cumulative Fractions

Figure 4